Exposure to enriched environment modulates the synaptic vesicle cycle in mice with spinal cord injury

Jeehyun Yoo

Department of Medicine

The Graduate School, Yonsei University

Exposure to enriched environment modulates the synaptic vesicle cycle in mice with spinal cord injury

Jeehyun Yoo

Department of Medicine

The Graduate School, Yonsei University

Exposure to enriched environment modulates the synaptic vesicle cycle in mice with spinal cord injury

Directed by Professor Ji Cheol Shin

The Doctoral Dissertation
submitted to the Department of Medicine,
the Graduate School of Yonsei University
in partial fulfillment of the requirements
for the degree of Doctor of Philosophy

Jeehyun Yoo

December 2021

This certifies that the Doctoral Dissertation of Jeehyun Yoo is approved.

Thesis Supervisor: Ji Cheol Shin

Thesis Committee Member#1: Sung-Rae Cho

Thesis Committee Member#2: Kil-Byung Lim

Thesis Committee Member#3: Se Hoon Kim

Thesis Committee Member#4: Hyun Seok Kim

The Graduate School
Yonsei University

December 2021

ACKNOWLEDGEMENTS

This thesis would not have been possible without the inspiration and support of wonderful individuals — my thanks and appreciation to all of them for being part of this journey and making this thesis possible.

I owe my deepest gratitude to my supervisor, Professor Ji Cheol Shin. He was the source of inspiration in the field of rehabilitation, and he encouraged me to pursue a specialty in spinal cord rehabilitation. You are the greatest mentor of my life.

I express my warmest gratitude to my associate supervisor, Professor Sung-Rae Cho. His guidance into the world of molecular biology has been a valuable input for this thesis. I also want to express my gratitude to my associate supervisors, Professor Kil-Byung Lim, Professor Se Hoon Kim, and Professor Hyun Seok Kim. They offered their support in many different ways, especially towards completing this thesis. Their commitment to the study was a significant influence in shaping many of the concepts presented in this thesis.

I also want to show my appreciation to Ahreum Baek for her support and her generosity in sharing her expertise and experiences throughout this research. My friends, YH and HY, thanks for your emotional support and encouragement, and I'm pleased to be a friend with you.

Finally, I express my deep and sincere gratitude to my parent and parent in-laws for their continuous and unparalleled love, help, and support. My mother has been taking care of her granddaughters while I was working on my thesis. Without your support, mom, this thesis would not have been completed. To my father, who is often left alone at home because my mother is away at my place: I sincerely love you. I also thank my brother, Jeeho Yoo, for helping with my English. I am grateful to my beloved husband, Yoonsik Jee, for his support and understanding. To my twin daughters, Sowon and Soyoon Jee: You gave me the precious gift of being a mother. I love you all so much.

<TABLE OF CONTENTS>

LIST OF FIGURES

LIST OF TABLES

ABSTRACT

Exposure to enriched environment modulates the synaptic vesicle cycle in mice with spinal cord injury

Jeehyun Yoo

Department of Medicine
The Graduate School, Yonsei University

(Directed by Professor Ji Cheol Shin)

An enriched environment (EE) consists of multiple mice in a large cage to increase social interaction and contains various toys, tunnels, shelters, and running wheels to increase locomotor activity. Exposure to an EE is a suitable method for inducing activity-dependent plasticity, and it is considered a similar condition with rehabilitation training in humans. Almost studies examining the effects of EE in the brain injury model revealed postsynaptic plasticity, and there is a lack of published research about presynaptic plasticity in gene expression level after EE exposure.

Therefore, the aims of this study are (1) to identify gene expression profile that is focused on synaptic vesicle cycle (SVC) at the different time points after SCI using RNA-sequencing and, (2) to identify whether EE could lead the presynaptic plasticity by modulating of SVC in spinal cord injured mice.

We performed RNA-sequencing and transcriptome analysis to characterize global gene expression after SCI at the different time points (two weeks and eight weeks after injury) compared with the sham (laminectomy) group. Differentially

expressed genes (DEGs), the result of transcriptome analysis, was then analyzed by a program Database of Annotation Visualization and Integrated Discovery which yielded the Kyoto Encyclopedia of Genes and Genomes (KEGG) pathway. And SCI mice were randomly assigned to either EE (SCI-EE) or standard cages (SCI-Control) for 2 or 8 weeks.

In transcriptome analysis results, we found 515 up-regulated and 128 down-regulated genes 2 weeks after SCI. Eight weeks after SCI, 1,073 up-regulated and 666 down-regulated genes were found. In particular, the SVC pathway was significantly down-regulated in both time points. To identify whether EE could modulate SVC, we conducted qRT-PCR and Western blot validation of down-regulated genes at 2 and/or 8 weeks after SCI, *Slc17a6*, *Rims1*, *Stxbp1*, *Unc13c*, *Cplx1*, *Cplx2*, *Snap25*, *Stx1b*, and *Dnm1*. The expression results were compared SCI-EE with SCI-Control. Immunohistochemistry for SNAP25 and Syntaxin 1 was also conducted. Basso Mouse Scale test, cylinder rearing test, and open field test were performed for the behavior assessment.

Overall, every examined gene expression in SCI-EE was higher than SCI-Control at 2 and 8 weeks after SCI. Especially at eight weeks after SCI, they showed significantly higher expression than SCI-Control. It either decreased or increased by 2 weeks. It means that exposure to EE modulates the SVC in SCI mice, and changes caused by EE exposure are more prominent when exposure is long duration. Neurobehavior evaluations, BMS, cylinder rearing test, and open field test showed dramatic improvement of functional recovery in eight weeks EE. Based on these results, we could assume that EE exposure leads to increased presynaptic activity (neurotransmitter uptake, docking, priming, fusion, and endocytosis) by modulating gene expression related to SVC.

Key words: enriched environment, spinal cord injuries, synaptic vesicles, neuronal plasticity, transcriptome, gene expression profiling

Exposure to enriched environment modulates the synaptic vesicle cycle in spinal cord injured mice

Jeehyun Yoo

Department of Medicine
The Graduate School, Yonsei University

(Directed by Professor Ji Cheol Shin)

I. INTRODUCTION

Spinal cord injury (SCI) results in motor and/or sensory impairment below the level of injury. The purpose of rehabilitation in SCI patients is to facilitate their functional recovery. Hebbian plasticity is use-dependent changes such as reinforcing active circuits and weakening inactive circuits in the central nervous system.[1] This activity-dependent plasticity is considered to be a mechanism of promoting functional recovery after rehabilitative training in SCI patients.[2-4]

An enriched environment (EE) consists of multiple mice in a large cage to increase social interaction and contains various toys, tunnels, shelters, and running wheels to increase locomotor activity. EE provides greater physical, somatosensory, cognitive, and social stimulation possibilities than the standard cage, which contains few mice with only food and water. Exposure to an EE is a suitable method for inducing activity-dependent plasticity, and it is considered a similar condition with rehabilitation training in humans. Several previous studies revealed functional improvement after exposure to EE in spinal cord injury animals.[5-9] An EE exposure leads to various plastic responses with increased

brain-derived neurotrophic factor (BDNF), increased presynaptic bouton density.[7,8]

Synaptic plasticity is the ability of synapses to modify their function, and it is considered the main component of activity-dependent plasticity. Presynaptic plasticity is the modification of neurotransmitter release by modulating synaptic vesicle cycle (SVC), especially fusion and priming, and postsynaptic plasticity is the modification of postsynaptic receptor.[10-13]

Almost studies examining the effects of EE in the brain injury model revealed postsynaptic plasticity.[14-16] Lee *et al.*[15] revealed that synaptic transmission and postsynaptic signal transduction genes were globally up-regulated. In contrast, those associated with reuptake by presynaptic neurotransmitter transporters were down-regulated after 2 mouths exposure to an EE in the adult mouse brain. There is no previous published study about altering gene expression profiling in SCI models by exposure to an EE but using treadmill training.[17] Treadmill training also increased the expression of genes involved in postsynaptic plasticity and angiogenesis.

There is a lack of published studies about presynaptic plasticity in gene expression level after EE exposure. However, it was reported in the studies about the spontaneous recovery of the SCI model. *Synapsin I, Synaptogyrin,* and *Synaptotagmin,* which are related to SVC, were up-regulated in that studies.[18,19] In contrast, these genes and other genes are associated with SVC (*SNAP25*, *Stxbp1*, *Sv2b*) are known as down-regulation during the acute phase of SCI.[20-24]

Therefore, the aims of this study are (1) to identify gene expression profile that is focused on SVC at the different time points after SCI using RNA-sequencing and (2) to identify whether EE could lead the presynaptic plasticity by modulating SVC in spinal cord injured mice.

II. MATERIALS AND METHODS

Animal

CD-1 (ICR) mice were housed in a facility accredited by the Association for Assessment and Accreditation of Laboratory Animal Care (AAALAC) for all animal experiments. The experimental procedure was approved by the Institutional Animal Care and Use Committee (IACUC) of Yonsei University Health System (permit number: 2016-0214). Seven weeks of age male mice (Orient Bio, Gyeonggi-do, South Korea) were used for this study.

Spinal cord contusion

Animals were anesthetized with ketamine (100 mg/kg ip) and xylazine (10 mg/kg ip) mixture. After anesthesia, the absence of blink and withdrawal reflexes were ensured. Body temperature was maintained at 37°C in a hypoxic chamber. Mice received a dorsal laminectomy at the 9th thoracic vertebral (T9) level to expose the spinal cord and then a moderate T9 contusive injury by the Infinite Horizons (IH) device (Precision Systems and Instrumentation, Lexington, NY, USA) to a moderate force of 70 kdyn in Figure 1(A). The sham group mice received only a dorsal laminectomy without contusive injury in Figure 1(B). Afterward, the wound was sutured in layers. Post-operative care consisted of manual bladder expression twice a day until automatic voiding returned spontaneously, which was generally around ten days.

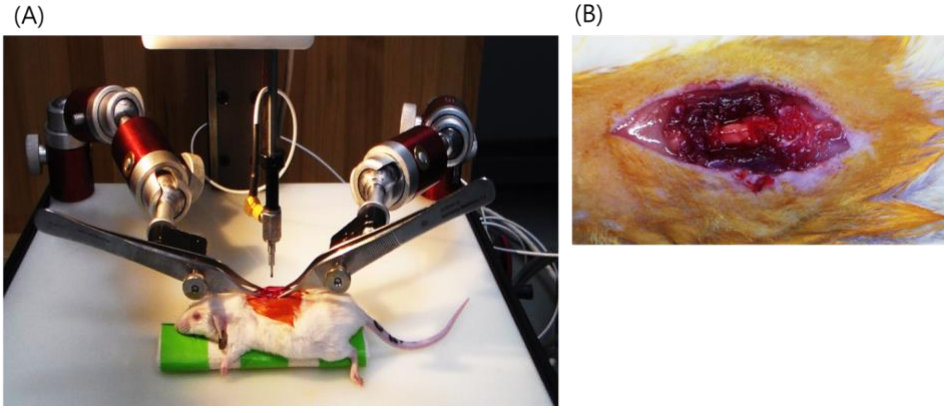

Figure 1. Production of SCI. (A) T9 region of the spinal cord of mice was injured by IH device. (B) Laminectomy was performed in the sham group.

RNA preparation

Two or 8 weeks after the operation, the mice were anesthetized again with a mixture of ketamine (100 mg/kg ip) and xylazine (10 mg/kg ip). They perfused transcardially with normal saline for isolation of injured spinal cords. These tissues were frozen at -70°C and processed for RNA isolation.

According to the manufacturer's instructions, total RNA was isolated from spinal cords obtained from SCI groups and sham groups using Trizol (Thermo Fisher Scientific, Massachusetts, USA**)** according to the *manufacturer's* instructions.[25] The quantity and purity of RNA were confirmed by a Nanodrop spectrophotometer (Thermo Fisher Scientific, Massachusetts, USA).

RNA-sequencing and transcriptome data analysis

RNA sequencing was performed at Macrogen Inc. (Seoul, South Korea) using HiSequation 2000 platform (Illumina, Sandiego, USA). The procedure for RNA sequencing was described in previous studies.[26,27]

Enriched KEGG pathway analysis

We used the database for annotation, visualization, and integrated discovery

(DAVID) software (http://david.abcc.ncifcrf.gov/) version 6.8[28] and KEGG Mapper version 2.8[29] (http://www.genome.jp/kegg/mapper) to identify enriched Kyoto Encyclopedia of Genes and Genomes (KEGG) pathways for differentially expressed genes (DEGs).

Enriched environment

A schematic timeline of this experiment is provided in Figure 2A. The Control group was housed in the standard cages (27 × 22.5 × 14 cm3) with three to five mice per cage for 2 or 8 weeks (Figure 2B). On the other hand, the enriched environment (EE) group was housed for 2 or 8 weeks in a large cage (86 × 76 × 31 cm3) which contains novel objects, such as tunnels, shelters, toys, and running wheels for voluntary exercise, and allowing for social interaction with 12 to 15 mice per cage (Figure 2C) as previous studies.[15,30-33]

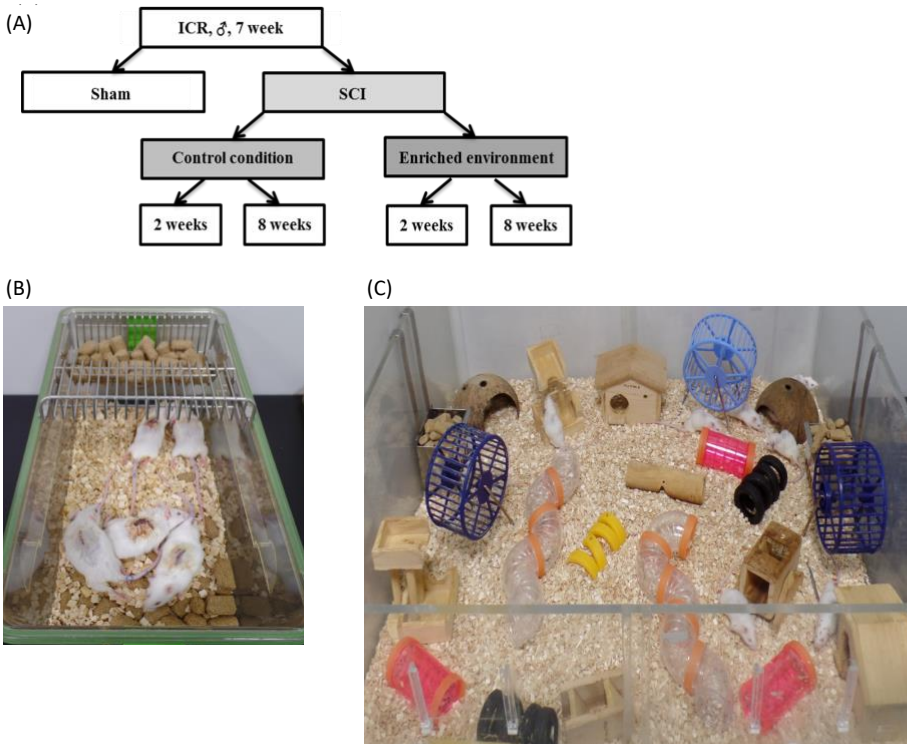

Figure 2. Experimental design. (A) The experimental scheme of this study. At 7 weeks of male CD-1(ICR) mice with spinal cord contusion, randomly assigned to either standard condition (indicated as control) or enriched environmental condition (indicated as EE). (B) The Control group was housed in the standard cage for 2 or 8 weeks. (C) EE group was housed in a large cage that contained novel objects, such as tunnels, shelters, toys, and running wheels for voluntary exercise and allowing for social interaction for 2 or 8 weeks.

Quantitative Real-Time Reverse Transcription Polymerase Chain Reaction (qRT-PCR)

The qRT-PCR was conducted to validate the transcriptome analysis. ACCORDING TO THE MANUFACTURER'S INSTRUCTIONS, total RNA was reverse-transcribed into cDNA using ReverTra Ace® qPCR RT Master Mix with gDNA Remover (Toyobo, Osaka, Japan). The mRNA expression for genes

of interest was profiled using qPCRBIO SyGreen Mix Hi-ROX (PCR BIOSYSTEMS, London, UK) in a StepOnePlus Real-Time PCR System (Applied Biosystems, Foster City, USA). Data analysis was performed using the 2-ΔΔ*CT* method.[34] Primers used for qRT-PCR were described in Table 1.

Table 1. Primers used for qRT-PCR

Gene symbol	Forward primer (5'→3')	Reverse primer (5'→3')
Slc17a6	GCT GGA AAA TCC CTC GGA CA	GCA TAG CGG AGC CTT CT
Rims1	CCA GAG CAA AAC GAG GAC GA	TTG TCG GTG CGT CCT TTC TC
Stxbp1	CGG TCC CCG CCT CAT TAT TT	GCA GTT TCT GTG GGG TGA GA
UNC13c	TGG GAA AGA GCT AGA CCC TGA	CGC ACT GTT CTT ATT CG
Cplx1	AAG TAC GCC AAG ATG GAG GC	GGG ATA GCC TTC TTG GGT CG
Cplx2	AGC CCT GGA ACA GCC CT	GCG GCC CTG GCA GAT ATT
SNAP25	GGA TGA GCA AGG CGA ACA AC	TCC TGA TTA TTG CCC CAG GC
Stx1B	AGC TGC GGA GTG CGA AAG A	GTC TTC TCA TCG GGG TTG GG
DNM1	ATC GAG GGT TCT GGA GAC CA	AAG CGA GGT CAG GTG TGA AG
GAPDH	CAT CAC TGC CAC CCA GAA GAC TG	ATG CCA GTG AGC TTC CCG TTC AG

Slc17a6; Solute carrier family 17 (sodium-dependent inorganic phosphate cotransporter), member 6, *Rims1*; Regulating synaptic membrane exocytosis 1, *Stxbp1*; Syntaxin binding protein 1, *UNC13c* ; Unc-13 homolog C , *Cplx1*; Complexin 1, *Cplx2*; Complexin 2, *SNAP25*; Synaptosomal-associated protein 25, *Stx1B* ; Syntaxin 1B, *DNM1*; Dynamin-1, *GAPDH* ; Glyceraldehyde 3-phosphate dehydrogenase.

Western blot

Gene expression confirmation was validated by qRT-PCR. For qRT-PCR, 50 μg of extracted proteins were dissolved in RIPA buffer, boiled for 5 min, and loaded onto 4–12% Bis-Tris gels. The separated proteins were then blotted onto polyvinylidene difluoride membranes (Amersham Pharmacia Biotech, Little Chalfont, UK) in 20% (vol/vol) methanol in NuPage Transfer Buffer (Invitrogen) in 4°C. The membranes were blocked for 1 h in Tris-buffered saline (TBS) containing 5% skim milk (Difco; BD Biosciences, Oxford, UK), washed three times with TBS containing 0.01% Tween 20 (TBST) for 10 min, and incubated overnight at 4°C with first antibodies specific to the target proteins. The first antibodies are Slc17A6, Munc18-1, SNAP25, Dynamin 1 (1:1000; Abcam, Cambridge, England), Rims1/2, Syntaxin, Actin (1:1000; Santa Cruz Biotechnology, Santa Cruz, USA) and Complexin-1/2 (1:1000; Cell Signaling Technology, Danvers, USA). The next day, the blots were washed 3 times with TBS with Tween 20 and incubated for 1 hour with horse-radish peroxidase-conjugated secondary antibodies (1:4000; Santa Cruz) at room temperature. After washing the blots three times with TBST, the blots were visualized with an enhanced chemiluminescence detection system (Amersham Pharmacia Biotech, Little Chalfont, UK).

Neurobehavior assessment

A. Basso Mouse Scale (BMS) test

BMS test was a validated scale used to monitor the progress of hind-limb functional recovery following SCI. The scale ranged from 0 (no ankle movement) to 9 (complete functional recovery) points. BMS scores were recorded at 3, 7, 14-, 28-, 42-, and 56-days following SCI by two independent examiners blind to the experimental conditions. The hind-limb motion was used to assess coordinated movement and stepping. When differences in the BMS score between the right and left hind limbs were observed, the average of the two scores was used.

B. Cylinder rearing test

When a mouse was placed in the cylinder, it reared spontaneously and used its forepaws for support. While the mouse was rearing, the number of times each forelimb contacted the cylinder wall (Jeung Do B&P, Seoul, Korea) was counted over five minutes.

C. Open field test

The open field test evaluates locomotor activity and spontaneous exploration in the novel environment. Activity monitoring was conducted in a square area measuring 30 x 30 x 30 cm^3. The area's floor was divided into 16 sections. The four inner sectors represented the center, while the 12 outer sectors were defined as the periphery. Mice were placed individually into the area's periphery and were allowed to explore freely for 25 minutes while being monitored with a video camera. The data were analyzed with the Smart Vision 2.5.21 (Panlab, Barcelona, Spain) video tracking system.

Immunohistochemistry

Animals were euthanized and perfused transcardially with 4% paraformaldehyde in 0.1 M phosphate buffer, Ph 7.4. Spinal cords were post-fixed 1 hour, followed by cryoprotection in 30% sucrose in Tris-buffered saline containing 0.02% sodium azide. Harvested spinal cord tissue was cryosectioned with a slice thickness of 10 μM along with the longitude, and immunohistochemistry staining was performed on four sections. For double immunofluorescence labeling, sections were stained with primary antibodies against rabbit anti-SNAP25 (1:400, Abcam), mouse anti-Syntaxin 1 (1:400, Santacruz), and secondary antibodies such as Alexa Flour 488 goat anti-rabbit (1:400, Invitrogen), Alexa Flour 594 anti-mouse (1:400 Invitrogen). Stained sections were mounted on glass slides with fluorescent mounting medium containing 4'6-diamidino-2-phenylindole (DAPI; Vectorshield, Vector, Burlingame, CA, USA). Stained sections were

analyzed using confocal microscopy (LSM700, Ziess, Gottingen, Germany).

Statistical analysis

All data were expressed as mean ± standard error of the mean (SEM). Statistical analyses were performed using Statistical Package for Social Sciences (SPSS) (SPSS Inc, Chicago, IL, USA) version 23.0. The comparison of variables between two groups was analyzed with Student's *t*-test. The variables among the groups were analyzed with a one-way analysis of variance (ANOVA) followed by a Bonferroni *post-hoc* test. A *p-value* <0.05 was considered statistically significant.

III. RESULTS

Analysis of the differentially expressed genes

The transcriptome analysis was conducted to identify differentially expressed genes (DEGs) in SCI compared to the sham group. At 2 weeks after SCI, 17,155 transcripts were differentially expressed compared to the sham group. Among that transcripts, 515 transcripts were 1.5-fold higher and 128 transcripts were -1.5-fold lower than the sham group (Figure 3A). Similarly, at 8 weeks after SCI, 17,048 transcripts were differentially expressed. Among that transcripts, 1,073 transcripts were 1.5-fold higher and 666 transcripts were -1.5-fold lower than the sham group (Figure 3B).

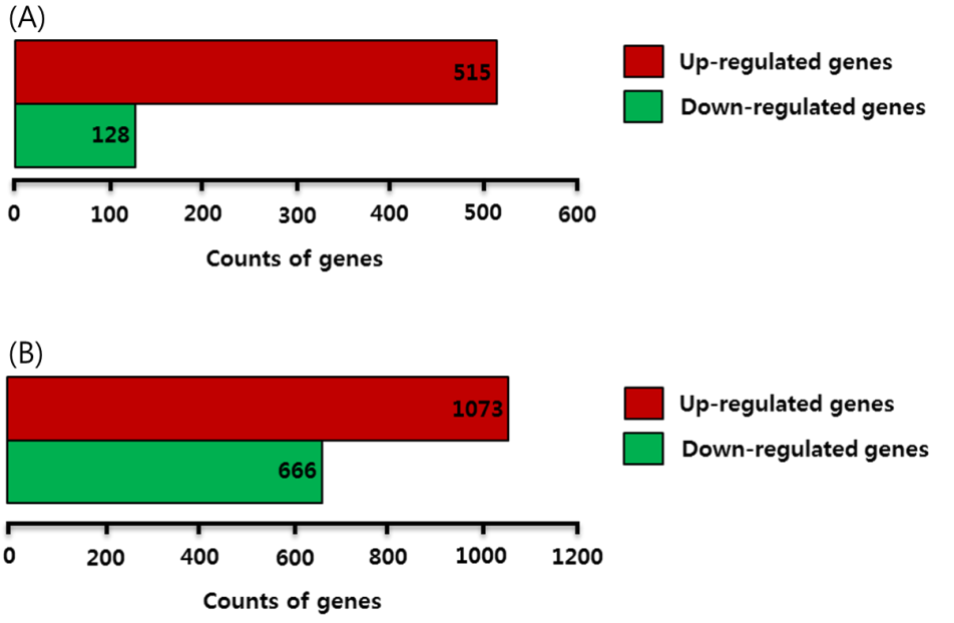

Figure 3. Gene expression profile by transcriptome analysis of the SCI compared to the sham group. (A) Bar graphs show the number of DEGs with fold change ≥ |1.5| in the SCI at 2 weeks after injury. (B) Bar graphs show the number of DEGs with fold change ≥ |1.5| in the SCI at 8 weeks after injury. The red bar indicated up-regulated genes, and the green bar indicated down-regulated genes.

Enriched KEGG pathway analysis

Compared to the sham group, up- and down-regulated DEGs of SCI at 2 or 8 weeks after injury were classified with enriched KEGG pathways from DAVID software version 6.8.

Of the 51 enriched pathways in up-regulated DEGs at 2 weeks after SCI, the top ten were mmu05150:Staphylococcus aureus infection, mmu05140:Leishmaniasis, mmu05310:Asthma, mmu04672:Intestinal immune network for IgA production, mmu00531:Glycosaminoglycan degradation, mmu04612:Antigen processing and presentation, mmu05323:Rheumatoid arthritis, mmu05133:Pertussis, mmu05332:Graft-versus-host disease, and mmu04145:Phagosome (Table 2). Of

the 17 enriched pathways in down-regulated DEGs at 2 weeks after SCI, the top ten were mmu04610:Complement and coagulation cascades, mmu00270:Cysteine and methionine metabolism, mmu05143:African trypanosomiasis, mmu04975:Fat digestion and absorption, mmu01230: Biosynthesis of amino acids, mmu00350:Tyrosine metabolism, mmu00260: Glycine, serine and threonine metabolism, mmu04721:Synaptic vesicle cycle, mmu03320:PPAR signaling pathway, and mmu00010:Glycolysis / Gluconeogenesis (Table 3).

Of the 63 enriched pathways in up-regulated DEGs at 8 weeks after SCI, the top ten were mmu05150:Staphylococcus aureus infection, mmu00531:Glycosaminoglycan degradation, mmu05140:Leishmaniasis, mmu05323:Rheumatoid arthritis, mmu04380:Osteoclast differentiation, mmu05310:Asthma, mmu04610:Complement and coagulation cascades, mmu04672:Intestinal immune network for IgA production, mmu04142:Lysosome, and mmu05133:Pertussis (Table 4). Of the 45 enriched pathways in down-regulated DEGs at 8 weeks after SCI, the top ten were mmu04721:Synaptic vesicle cycle, mmu04723:Retrograde endocannabinoid signaling, mmu00250:Alanine, aspartate and glutamate metabolism, mmu05033:Nicotine addiction,mmu04727:GABAergic synapse, mmu04728:Dopaminergic synapse, mmu04971:Gastric acid secretion, mmu04930:Type II diabetes mellitus, mmu04970:Salivary secretion, and mmu04915:Estrogen signaling pathway (Table 5).

Among several pathways, the ‘SVC pathway’, which we focused on, was down-regulated in both SCI following 2 and 8 weeks compared to the sham group (Figure 4). At 2 weeks after SCI, *Slc17a6*, *Rims1*, *Stx1b*, and *Dnm1* were significantly down-regulated compared to the sham group. At 8 weeks after SCI, *Atp6v1b2, Slc32a1, Slc17a6, Slc18a3, Stxbp1, Rims1*, *Unc13c, Stx1b, Cplx1, Cplx2, Snap25, Nsf, Dnm1* and *Dnm3* were significantly down-regulated compared to sham group. Especially, *Slc17a6*, *Rims1*, *Stx1b,* and *Dnm1* were

significantly down-regulated at 2 and 8 weeks after SCI compared to the sham group.

Table 2. Enriched KEGG pathways identified to be significantly up-regulated in 2 weeks post-SCI.

Term	Count	*p* value	Genes	Fold Enrichment
mmu05150:Staphylococcus aureus infection	20	3.71E-16	ICAM1, C3AR1, C4B, C3, FCGR4, H2-DMB1, ITGB2, H2-AB1, FCGR1, C1QC, ITGAM, H2-DMB2, FCGR3, C1QA, C1QB, FCGR2B, H2-EB1, CFH, H2-AA, H2-DMA	12.157
mmu05140:Leishmaniasis	20	7.42E-14	PTPN6, NCF2, NCF1, C3, NCF4, TLR2, FCGR4, H2-DMB1, ITGB2, H2-AB1, FCGR1, ITGAM, TGFB1, H2-DMB2, FCGR3, FOS, CYBA, H2-EB1, H2-AA, H2-DMA	9.498
mmu05310:Asthma	7	9.56E-05	H2-EB1, H2-DMB1, FCER1G, H2-AA, H2-AB1, H2-DMA, H2-DMB2	8.865
mmu04672:Intestinal immune network for IgA production	10	6.54E-06	CD86, LTBR, CXCR4, H2-EB1, H2-DMB1, H2-AA, H2-AB1, H2-DMA, H2-DMB2, TGFB1	7.237
mmu00531:Glycosaminoglycan degradation	5	0.004	NAGLU, HPSE, GUSB, HEXA, HEXB	7.237
mmu04612:Antigen processing and presentation	19	9.33E-11	H2-Q2, H2-K1, H2-D1, IFI30, H2-DMB1, H2-AB1, HSPA1A, CTSS, HSPA1B, CD74, H2-Q8, H2-DMB2, B2M, CTSL, TAP1, H2-EB1, H2-AA, CTSB, H2-DMA	7.042
mmu05323:Rheumatoid arthritis	19	9.33E-11	TCIRG1, ICAM1, CCL3, CCL2, TLR2, ACP5, H2-DMB1, ITGB2, H2-AB1, CCL5, TGFB1, H2-DMB2, FOS, CCL12, CTSL, CD86, H2-EB1, H2-AA, H2-DMA	7.042
mmu05133:Pertussis	16	1.16E-08	C3, C4B, LY96, ITGB2, SERPING1, C1QC,	6.572

mmu05332:Graft-versus-host disease	11	5.62E-06	ITGAM, C1QA, FOS, C1QB, ITGA5, IRF8, PYCARD, IRF1, CASP1, CD14 H2-K1, H2-Q2, CD86, H2-EB1, H2-D1, H2-DMB1, H2-AA, H2-AB1, H2-DMA, H2-DMB2, H2-Q8	6.429
mmu04145:Phagosome	36	1.15E-18	MSR1, C3, TLR2, H2-D1, ITGB5, ITGB2, ITGAM, TAP1, TUBB6, TCIRG1, H2-Q2, H2-K1, NCF2, NCF1, NCF4, FCGR4, H2-DMB1, COLEC12, H2-AB1, CTSS, FCGR1, H2-Q8, H2-DMB2, FCGR3, CYBA, CTSL, CYBB, SEC61B, CD36, FCGR2B, ITGA5, H2-EB1, H2-AA, CLEC7A, H2-DMA, CD14	6.288
mmu04380:Osteoclast differentiation	26	2.04E-13	FOSL2, SPI1, ACP5, TGFB1, FOS, TNFRSF1A, PIK3R5, CSF1R, SYK, BLNK, TYROBP, NCF2, NCF1, SOCS3, TGFBR1, NCF4, FCGR4, FCGR1, JUNB, FCGR3, PIRB, CYBA, CYBB, FCGR2B, TREM2, LCP2	6.272
mmu04640:Hematopoietic cell lineage	17	9.59E-09	ANPEP, FCGR1, ITGAM, CD9, CD37, CD36, CD44, ITGA5, CD34, CD33, H2-EB1, CSF3R, CD22, CSF2RA, IL3RA, CD14, CSF1R	6.151
mmu05330:Allograft rejection	11	1.13E-05	H2-K1, H2-Q2, CD86, H2-EB1, H2-D1, H2-DMB1, H2-AA, H2-AB1, H2-DMA, H2-DMB2, H2-Q8	5.970
mmu05144:Malaria	9	1.44E-04	HBA-A1, CCL12, ICAM1, CCL2, CD36, TLR2, ITGB2, HBB-BT, TGFB1	5.699
mmu04142:Lysosome	22	3.12E-10	TCIRG1, NAGLU, CTSZ, PLA2G15, HEXA, GUSB, HEXB, ACP5, CTSA, CTSS, CD63, DNASE2A, SLC11A1, CTSL, CD68, LAPTM5,	5.481

			CTSE, CTSD, CTSC, CTSB, MAN2B1, CTSH	
mmu04940:Type I diabetes mellitus	11	2.86E-05	H2-K1, H2-Q2, CD86, H2-EB1, H2-D1, H2-DMB1, H2-AA, H2-AB1, H2-DMA, H2-DMB2, H2-Q8	5.392
mmu05416:Viral myocarditis	14	1.42E-06	H2-Q2, H2-K1, ICAM1, H2-D1, H2-DMB1, ITGB2, H2-AB1, H2-DMB2, H2-Q8, CD86, RAC2, H2-EB1, H2-AA, H2-DMA	5.386
mmu05152:Tuberculosis	31	4.98E-14	C3, TLR1, TLR2, ITGB2, CD74, TGFB1, ITGAM, TNFRSF1A, ITGAX, IL10RB, IL10RA, FCER1G, LBP, SYK, TCIRG1, CEBPB, FCGR4, H2-DMB1, H2-AB1, CTSS, FCGR1, H2-DMB2, FCGR3, LSP1, FCGR2B, H2-EB1, H2-AA, CTSD, CLEC7A, H2-DMA, CD14	5.353
mmu04662:B cell receptor signaling pathway	12	1.47E-05	FOS, PTPN6, FCGR2B, LYN, RAC2, CD22, PIK3R5, INPP5D, CD72, VAV1, BLNK, SYK	5.210
mmu04610:Complement and coagulation cascades	13	5.68E-06	C3AR1, A2M, C4B, C3, SERPING1, C1QC, PLAUR, C1QA, C1QB, SERPINE1, CFH, PROS1, PLAU	5.199
mmu04666:Fc gamma R-mediated phagocytosis	14	2.90E-06	PTPRC, ARPC1B, DOCK2, RAC2, FCGR2B, LYN, NCF1, HCK, PIK3R5, INPP5D, WAS, FCGR1, VAV1, SYK	5.066
mmu04620:Toll-like receptor signaling pathway	16	8.53E-07	FOS, CCL3, CD86, IRF5, LY96, IRF7, TLR1, TLR2, PIK3R5, LBP, CCL5, TLR7, CCL4, CD14, SPP1, CXCL10	4.815
mmu05134:Legionellosis	9	4.89E-04	C3, PYCARD, TLR2, ITGB2, HSPA1A, HSPA1B, CASP1, ITGAM, CD14	4.799

mmu04623:Cytosolic DNA-sensing pathway	10	2.15E-04	IFI202B, TMEM173, IRF7, PYCARD, CCL5, CASP1, CCL4, AIM2, ZBP1, CXCL10	4.749
mmu05142:Chagas disease (American trypanosomiasis)	16	1.10E-06	GNA15, CCL3, CCL2, C3, TGFBR1, TLR2, CCL5, C1QC, TGFB1, C1QA, FOS, TNFRSF1A, C1QB, CCL12, SERPINE1, PIK3R5	4.721
mmu05320:Autoimmune thyroid disease	11	9.49E-05	H2-K1, H2-Q2, CD86, H2-EB1, H2-D1, H2-DMB1, H2-AA, H2-AB1, H2-DMA, H2-DMB2, H2-Q8	4.709
mmu05321:Inflammatory bowel disease (IBD)	9	6.21E-04	H2-EB1, TLR2, H2-DMB1, H2-AA, IL2RG, H2-AB1, H2-DMA, H2-DMB2, TGFB1	4.636
mmu05145:Toxoplasmosis	17	7.10E-07	IRGM1, LY96, TLR2, H2-DMB1, H2-AB1, HSPA1A, HSPA1B, TGFB1, H2-DMB2, TNFRSF1A, IGTP, IL10RB, IL10RA, H2-EB1, H2-AA, PIK3R5, H2-DMA	4.573
mmu04064:NF-kappa B signaling pathway	14	1.48E-05	ICAM1, LTBR, LYN, LY96, CCL4, TNFRSF1A, BCL2A1D, BCL2A1B, BCL2A1A, LBP, CD14, PLAU, BLNK, SYK	4.387
mmu04650:Natural killer cell mediated cytotoxicity	14	3.51E-05	PTPN6, ICAM1, FCGR4, ITGB2, VAV1, HCST, CD48, RAC2, FCER1G, PIK3R5, SYK, TYROBP, LCP2, SH3BP2	4.052
mmu04668:TNF signaling pathway	14	5.23E-05	ICAM1, CCL2, CEBPB, SOCS3, IFI47, CCL5, JUNB, CXCL10, TNFRSF1A, CCL12, FOS, TNFRSF1B, BCL3, PIK3R5	3.904
mmu05132:Salmonella infection	10	9.56E-04	FOS, ARPC1B, CCL3, PYCARD, LBP, CASP1, FLNC, WAS, CCL4, CD14	3.897
mmu04062:Chemokine signaling pathway	24	8.97E-08	CCL3, CCL2, FGR, LYN, NCF1, CCR1, HCK, GM20878, CCL9, CCL5, WAS, CCL4, VAV1,	3.722

			CCL6, CXCL10, CCL12, DOCK2, GNGT2, RAC2, CXCR4, CXCL16, CX3CR1, PIK3R5, GM21586	
mmu04664:Fc epsilon RI signaling pathway	8	0.007	LYN, RAC2, FCER1G, PIK3R5, INPP5D, VAV1, SYK, LCP2	3.576
mmu05164:Influenza A	20	2.85E-06	ICAM1, CCL2, SOCS3, H2-DMB1, H2-AB1, HSPA1A, HSPA1B, CCL5, TLR7, H2-DMB2, CXCL10, CCL12, TNFRSF1A, IRF7, H2-EB1, PYCARD, H2-AA, PIK3R5, CASP1, H2-DMA	3.555
mmu04670:Leukocyte transendothelial migration	14	1.55E-04	CYBA, ICAM1, CYBB, NCF2, RAC2, NCF1, CXCR4, NCF4, MYLPF, ITGB2, PIK3R5, MMP2, VAV1, ITGAM	3.517
mmu04060:Cytokine-cytokine receptor interaction	28	2.47E-08	CCL3, CCL2, OSMR, TNFRSF12A, CSF2RB2, CCR1, CCL5, CCL4, TGFB1, CXCL10, TNFRSF1A, TNFRSF1B, IL10RB, CXCR4, IL10RA, CSF2RB, CSF3R, IL2RG, CSF2RA, CSF1R, LTBR, TGFBR1, GM20878, CCL12, CXCL16, CX3CR1, GM21586, IL3RA	3.474
mmu04512:ECM-receptor interaction	10	0.002	CD36, CD44, ITGA5, TNC, COL3A1, COL1A2, ITGB5, COL1A1, FN1, SPP1	3.454
mmu04514:Cell adhesion molecules (CAMs)	18	2.06E-05	H2-Q2, H2-K1, PTPRC, ICAM1, H2-D1, H2-DMB1, ITGB2, H2-AB1, ITGAM, H2-Q8, H2-DMB2, CD86, GLYCAM1, CD34, H2-EB1, CD22, H2-AA, H2-DMA	3.377
mmu05205:Proteoglycans in cancer	21	9.88E-06	PTPN6, HCLS1, LUM, TLR2, ITGB5, FLNC, CD63, MMP2, TGFB1, PLAUR, CTSL, CD44, ITGA5, HPSE, COL1A2, HBEGF, PIK3R5, COL1A1, MYC, PLAU, FN1	3.144

mmu05146:Amoebiasis	12	0.002	GNA15, COL3A1, COL1A2, TLR2, HSPB1, PIK3R5, ITGB2, COL1A1, ITGAM, TGFB1, CD14, FN1	3.117
mmu05322:Systemic lupus erythematosus	15	3.13E-04	C3, C4B, FCGR4, H2-DMB1, H2-AB1, FCGR1, C1QC, H2-DMB2, C1QA, C1QB, CD86, H2-EB1, H2-AA, H2-DMA, HIST1H4H	3.101
mmu05168:Herpes simplex infection	21	1.42E-05	H2-Q2, H2-K1, CCL2, SOCS3, C3, TLR2, H2-D1, H2-DMB1, H2-AB1, CCL5, CD74, H2-Q8, H2-DMB2, FOS, CCL12, TNFRSF1A, IRF7, TAP1, H2-EB1, H2-AA, H2-DMA	3.069
mmu05202:Transcriptional misregulation in cancer	16	3.41E-04	CEBPA, CEBPB, SPI1, FCGR1, ITGAM, CD86, BCL2A1D, NUPR1, BCL2A1B, BCL2A1A, LYL1, MYC, HPGD, PLAU, CD14, CSF1R	2.930
mmu04611:Platelet activation	12	0.004	TBXAS1, LYN, VAMP8, FERMT3, COL3A1, COL1A2, FCER1G, PIK3R5, COL1A1, APBB1IP, SYK, LCP2	2.784
mmu04630:Jak-STAT signaling pathway	13	0.003	PTPN6, OSMR, SOCS3, IL10RB, CSF2RB2, IL10RA, CSF2RB, CSF3R, PIK3R5, IL2RG, MYC, CSF2RA, IL3RA	2.725
mmu05169:Epstein-Barr virus infection	18	6.67E-04	H2-Q2, H2-K1, ICAM1, LYN, FGR, VIM, H2-D1, SPI1, HSPA1A, HSPA1B, H2-Q8, CD44, IL10RB, IL10RA, HSPB1, PIK3R5, MYC, SYK	2.545
mmu05166:HTLV-I infection	23	1.07E-04	H2-Q2, H2-K1, ICAM1, TSPO, LTBR, TGFBR1, SPI1, H2-D1, H2-DMB1, ITGB2, H2-AB1, H2-Q8, TGFB1, H2-DMB2, FOS, TNFRSF1A, ATF3, H2-EB1, H2-AA, IL2RG,	2.515

			PIK3R5, H2-DMA, MYC	
mmu04510:Focal adhesion	14	0.018	PARVG, RAC2, ITGA5, TNC, COL3A1, COL1A2, ITGB5, MYLPF, PIK3R5, COL1A1, FLNC, VAV1, SPP1, FN1	2.056

These pathways are statistically significant (p <0.05).

Table 3. Enriched KEGG pathways identified to be significantly down-regulated in 2 weeks post-SCI

Term	Count	*p* value	Genes	Fold Enrichment
mmu04610:Complement and coagulation cascades	12	3.37E-12	KNG1, MBL2, FGG, FGA, SERPINA1B, SERPINA1A, FGB, SERPINA1D, F2, SERPINA1C, SERPINA1E, PLG	21.767
mmu00270:Cysteine and methionine metabolism	4	0.003	MAT1A, SDS, BHMT, TAT	13.786
mmu05143:African trypanosomiasis	3	0.026	HBA-A2, PLCB4, APOA1	11.816
mmu04975:Fat digestion and absorption	3	0.030	APOA4, APOA1, FABP1	10.883
mmu01230:Biosynthesis of amino acids	6	2.17E-04	ARG1, MAT1A, SDS, ALDOB, CPS1, TAT	10.604
mmu00350:Tyrosine metabolism	3	0.031	ADH1, TAT, HPD	10.604
mmu00260:Glycine, serine and threonine metabolism	3	0.033	SDS, BHMT, GNMT	10.339
mmu04721:Synaptic vesicle cycle	4	0.010	SLC17A7, RIMS1, STX1B, DNM1	8.894

mmu03320:PPAR signaling pathway	5	0.002	APOA2, APOA1, APOC3, FABP1, PCK1	8.616
mmu00010:Glycolysis / Gluconeogenesis	4	0.011	ADH1, ALDOB, FBP1, PCK1	8.355
mmu05150:Staphylococcus aureus infection	3	0.049	MBL2, FGG, PLG	8.271
mmu00140:Steroid hormone biosynthesis	4	0.024	CYP2D10, CYP3A11, UGT2B5, CYP2D26	6.338
mmu00830:Retinol metabolism	4	0.025	ALDH1A2, ADH1, CYP3A11, UGT2B5	6.196
mmu04723:Retrograde endocannabinoid signaling	4	0.037	SLC17A7, PLCB4, RIMS1, KCNJ3	5.354
mmu01200:Carbon metabolism	4	0.049	SDS, ALDOB, FBP1, CPS1	4.754
mmu01130:Biosynthesis of antibiotics	6	0.018	ARG1, SDS, ALDOB, FBP1, TAT, PCK1	3.865
mmu01100:Metabolic pathways	17	0.014	CYP3A11, ALDOB, FBP1, CPS1, TAT, PCK1, ARG1, ALDH1A2, TDO2, PLCB4, ADH1, MAT1A, UOX, SDS, BHMT, UGT2B5, HPD	1.834

These pathways are statistically significant (p <0.05).

Table 4. Enriched KEGG pathways identified to be significantly up-regulated in 8 weeks post-SCI.

Term	Count	*p* Value	Genes	Fold Enrichment
mmu05150:Staphylococcus aureus infection	22	2.70E-13	ICAM1, C3AR1, C4B, C3, FCGR4, H2-DMB1, ITGB2, H2-AB1, FCGR1, C1QC, ITGAM, H2-DMB2, FCGR3, C1QA, C1RA, C1QB,	7.181
mmu00531:Glycosaminoglycan degradation	8	1.67E-04	FCGR2B, H2-EB1, CFH, H2-AA, C2, PTAFR GNS, ARSB, NAGLU, HPSE, GUSB, HEXA, HEXB, GALNS	6.218
mmu05140:Leishmaniasis	24	1.01E-12	PTPN6, NCF2, NCF1, C3, MARCKSL1, NCF4, FCGR4, TLR2, NFKBIA, H2-DMB1, ITGB2, H2-AB1, FCGR1, ITGAM, TGFB1, H2-DMB2, FCGR3, FOS, CYBA, JUN, H2-EB1, IL1B, H2-AA, IFNGR1	6.121
mmu05323:Rheumatoid arthritis	26	7.06E-12	CCL3, CCL2, CSF1, TLR2, ACP5, ITGB2, TNFSF13, CCL5, CXCL12, TGFB1, FOS, ATP6V0E, IL1B, ATP6V0D2, LTB, TCIRG1, ICAM1, H2-DMB1, H2-AB1, H2-DMB2,	5.175
mmu04380:Osteoclast differentiation	37	1.44E-15	CTSL, CCL12, CD86, JUN, H2-EB1, H2-AA IL1R1, CSF1, SPI1, ACP5, NFKBIA, NFKB2, TGFB1, BTK, FOS, TNFRSF1A, IL1B, PIK3R5, IFNGR1, CSF1R, TEC, BLNK, SYK, TYROBP, NCF2, NCF1, SOCS3, TGFBR1, NCF4, TGFBR2, FCGR4, FCGR1, SIRPA, JUNB, FCGR3, PIRB, CYBA, CYBB,	4.793
mmu05310:Asthma	7	0.003	FCGR2B, JUN, PLCG2, TREM2, LCP2 CCL11, H2-EB1, H2-DMB1, FCER1G, H2-AA,	4.760

			H2-AB1, H2-DMB2	
mmu04610:Complement and coagulation cascades	22	2.62E-09	PLAT, C3AR1, A2M, KNG2, C4B, C3, SERPING1, C1QC, PLAUR, C1QA, C1RA, C1QB, THBD, SERPINA1B, CD59A, SERPINA1D, SERPINE1, CFH, TFPI, C2, PROS1, PLAU	4.725
mmu04672:Intestinal immune network for IgA production	12	3.01E-05	ICOSL, CD86, LTBR, CXCR4, H2-EB1, H2-DMB1, H2-AA, TNFSF13, H2-AB1, CXCL12, H2-DMB2, TGFB1	4.663
mmu04142:Lysosome	33	7.72E-13	ARSB, NAGLU, LITAF, HEXA, HEXB, ACP5, CTSA, SLC11A1, CD68, LAPTM5, TPP1, NAGA, GALNS, MAN2B1, ATP6V0D2, TCIRG1, CLN3, CTSZ, LAPTM4A, PLA2G15, LIPA, GUSB, CTSS, CD63, DNASE2A, GNS, CTSL, NPC2, CTSE, CTSD, CTSC, CTSB, CTSH	4.415
mmu05133:Pertussis	19	3.06E-07	GNAI2, C3, C4B, ITGB2, SERPING1, C1QC, ITGAM, C1QA, FOS, C1QB, C1RA, ITGA5, JUN, IRF8, PYCARD, IRF1, IL1B, C2, CD14	4.191
mmu05332:Graft-versus-host disease	13	5.18E-05	H2-K1, H2-M3, H2-Q1, H2-D1, H2-DMB1, H2-AB1, H2-Q8, H2-DMB2, CD86, H2-EB1, IL1B, H2-AA, FAS	4.080
mmu05144:Malaria	12	1.14E-04	HBA-A1, CCL12, ICAM1, GYPC, SDC1, CCL2, TLR2, IL1B, ITGB2, THBS2, THBS3, TGFB1	4.080
mmu05134:Legionellosis	14	2.89E-05	CXCL1, C3, TLR2, NFKBIA, ITGB2, NFKB2, ITGAM, NAIP2, HSPA2, CASP8, NAIP5,	4.009

			PYCARD, IL1B, CD14	
mmu04612:Antigen processing and presentation	20	3.27E-07	H2-K1, H2-M3, H2-Q1, H2-D1, IFI30, H2-DMB1, H2-AB1, CTSS, CD74, H2-Q8, H2-DMB2, B2M, TAPBP, CTSL, HSPA2, TAP2, TAP1, H2-EB1, H2-AA, CTSB	3.981
mmu05142:Chagas disease (American trypanosomiasis)	25	8.06E-09	GNA15, CCL3, CCL2, GNAI2, C3, TGFBR1, TGFBR2, TLR2, NFKBIA, CCL5, C1QC, TGFB1, C1QA, FOS, CCL12, TNFRSF1A, C1QB, PLCB3, JUN, CASP8, SERPINE1, IL1B, PIK3R5, FAS, IFNGR1	3.961
mmu04145:Phagosome	42	2.21E-14	MSR1, C3, TLR2, H2-D1, ITGB5, ITGB2, ITGAM, C1RA, ATP6V0E, TAP2, TAP1, TUBB6, THBS2, ATP6V0D2, THBS3, TCIRG1, MRC1, H2-K1, H2-M3, NCF2, NCF1, NCF4, MRC2, H2-Q1, FCGR4, H2-DMB1, COLEC12, H2-AB1, CTSS, FCGR1, H2-Q8, H2-DMB2, FCGR3, CYBA, CTSL, CYBB, FCGR2B, ITGA5, H2-EB1, H2-AA, CLEC7A, CD14	3.940
mmu04512:ECM-receptor interaction	21	2.24E-07	TNXB, TNC, COL3A1, ITGB5, VTN, COL5A3, SDC4, COL5A2, SDC1, LAMB2, CD44, ITGA5, COL6A2, COL1A2, COL6A1, COL1A1, COL11A2, THBS2, THBS3, SPP1, FN1	3.895
mmu04640:Hematopoietic cell lineage	20	4.88E-07	IL1R1, CSF1, IL4RA, ANPEP, FCGR1, ITGAM, CD9, CD37, CD44, ITGA5, CD59A, CD33, H2-EB1, IL1B, CSF3R, CD22, CSF2RA,	3.886

			IL3RA, CD14, CSF1R	
mmu05321:Inflammatory bowel disease (IBD)	14	4.27E-05	IL21R, IL4RA, TLR2, H2-DMB1, H2-AB1, H2-DMB2, TGFB1, STAT6, JUN, H2-EB1, IL1B, H2-AA, IL2RG, IFNGR1	3.873
mmu04064:NF-kappa B signaling pathway	23	5.76E-08	TRAF1, ICAM1, IL1R1, LTBR, LYN, NFKBIA, NFKB2, CXCL12, CCL4, BTK, TNFRSF1A, BCL2A1D, BCL2A1B, BCL2A1A, RIPK1, PLCG2, IL1B, LBP, LTB, CD14, PLAU, SYK, BLNK	3.870
mmu04666:Fc gamma R-mediated phagocytosis	19	2.26E-06	PTPRC, LYN, NCF1, MARCKSL1, HCK, ASAP3, WAS, PRKCD, VAV1, FCGR1, ARPC1B, DOCK2, FCGR2B, RAC2, PLCG2, PIK3R5, MARCKS, INPP5D, SYK	3.692
mmu05152:Tuberculosis	39	3.80E-12	C3, TLR1, TLR2, ITGB2, TGFB1, CD74, ITGAM, TNFRSF1A, ITGAX, IL10RB, IL10RA, CASP8, IL1B, FCER1G, LBP, ATP6V0D2, IFNGR1, SYK, TCIRG1, MRC1, IRAK2, CEBPB, CARD9, CAMP, MRC2, FCGR4, H2-DMB1, H2-AB1, CTSS, FCGR1, H2-DMB2, FCGR3, LSP1, FCGR2B, H2-EB1, H2-AA, CTSD, CLEC7A, CD14	3.617
mmu05020:Prion diseases	7	0.012	EGR1, C1QA, C1QB, CASP12, IL1B, CCL5, C1QC	3.570
mmu04662:B cell receptor signaling pathway	15	6.83E-05	PTPN6, LYN, NFKBIA, VAV1, BTK, FOS, FCGR2B, RAC2, JUN, PLCG2, CD22, PIK3R5, INPP5D, SYK, BLNK	3.497
mmu05330:Allograft rejection	12	4.80E-04	H2-K1, CD86, H2-M3, H2-EB1, H2-Q1, H2-	3.497

			D1, H2-DMB1, H2-AA, H2-AB1, FAS, H2-DMB2, H2-Q8	
mmu04668:TNF signaling pathway	23	5.10E-07	TRAF1, CXCL1, ICAM1, CEBPB, CCL2, SOCS3, CSF1, NFKBIA, CCL5, JUNB, CXCL10, FOS, TNFRSF1A, CCL12, TNFRSF1B, JUN, RIPK1, CASP8, IL1B, BCL3, CREB3L1, PIK3R5, FAS	3.444
mmu04940:Type I diabetes mellitus	13	3.10E-04	H2-K1, H2-M3, H2-Q1, H2-D1, H2-DMB1, H2-AB1, H2-Q8, H2-DMB2, CD86, H2-EB1, IL1B, H2-AA, FAS	3.422
mmu04620:Toll-like receptor signaling pathway	21	2.31E-06	CCL3, TLR1, TLR2, NFKBIA, CCL5, CCL4, TLR7, CXCL10, FOS, IKBKE, CD86, IRF5, JUN, RIPK1, IRF7, CASP8, IL1B, PIK3R5, LBP, CD14, SPP1	3.394
mmu05340:Primary immunodeficiency	7	0.016	PTPRC, TAP2, TAP1, IL2RG, ADA, BLNK, BTK	3.360
mmu05416:Viral myocarditis	16	7.12E-05	H2-K1, ICAM1, H2-M3, H2-Q1, H2-D1, H2-DMB1, ITGB2, H2-AB1, H2-Q8, H2-DMB2, CD86, RAC2, CASP8, H2-EB1, H2-AA, SGCA	3.306
mmu05132:Salmonella infection	15	2.30E-04	CXCL1, FOS, PFN1, ARPC1B, CCL3, JUN, PYCARD, IL1B, LBP, FLNC, WAS, CCL4, IFNGR1, CD14, FLNA	3.139
mmu04670:Leukocyte transendothelial migration	23	3.24E-06	ICAM1, NCF2, GNAI2, NCF1, NCF4, SIPA1, ITGB2, MYL12A, CXCL12, VAV1, MMP2, ITGAM, CLDN14, MYL9, CYBA, CYBB, EZR, RAC2, PTK2B, CXCR4, PLCG2, PIK3R5, MSN	3.102

mmu04623:Cytosolic DNA-sensing pathway	12	0.002	IFI202B, IKBKE, TMEM173, RIPK1, IRF7, PYCARD, IL1B, NFKBIA, CCL5, CCL4, AIM2, CXCL10	3.060
mmu04060:Cytokine-cytokine receptor interaction	45	5.38E-11	IL1R1, CCL3, CCL2, CSF2RB2, IL6ST, OSMR, CSF1, IL4RA, IL21R, TNFSF13, PF4, CCL5, CXCL12, CCL4, CCL7, TGFB1, IL17RA, CXCL10, TNFRSF1A, TNFRSF1B, CLCF1, IL10RB, CXCR4, IL10RA, IL1B, CSF2RB, CSF3R, IL2RG, FAS, IL13RA1, LTB, CSF2RA, IFNGR1, CSF1R, LTBR, TGFBR1, TGFBR2, ACKR3, CCL11, OSM, CCL12, CNTF, CXCL16, CX3CR1, IL3RA	2.998
mmu05205:Proteoglycans in cancer	37	4.66E-09	LUM, TLR2, ITGB5, VTN, DCN, SDC4, MMP2, IQGAP1, TGFB1, WNT4, EZR, CD44, HPSE, RRAS, PIK3R5, MSN, FAS, WNT6, MYC, FN1, PTPN6, HCLS1, IGF1, IGF2, FLNC, CD63, FLNA, PLAUR, CTSL, FZD10, SDC1, ITGA5, PLCG2, COL1A2, HBEGF, COL1A1, PLAU	2.975
mmu04621:NOD-like receptor signaling pathway	10	0.006	CCL12, CCL2, CARD9, NAIP2, NAIP5, CASP8, PYCARD, IL1B, NFKBIA, CCL5	2.915
mmu05320:Autoimmune thyroid disease	12	0.004	H2-K1, CD86, H2-M3, H2-EB1, H2-Q1, H2-D1, H2-DMB1, H2-AA, H2-AB1, FAS, H2-DMB2, H2-Q8	2.759
mmu04611:Platelet activation	22	4.00E-05	TLN1, TBXAS1, GNAI2, LYN, FERMT3, COL3A1, MYL12A, COL5A3, APBB1IP, COL5A2, BTK, PLCB3, VAMP8, PLCG2, COL1A2, FCER1G, PIK3R5, COL1A1,	2.741

			COL11A2, MYLK, SYK, LCP2	
mmu04210:Apoptosis	10	0.010	TNFRSF1A, CSF2RB2, RIPK1, CASP12, CASP8, NFKBIA, CSF2RB, PIK3R5, FAS, IL3RA	2.720
mmu04062:Chemokine signaling pathway	32	8.06E-07	CXCL1, CCL3, CCL2, GNAI2, FGR, CCL9, NFKBIA, PF4, CCL5, CXCL12, CCL4, CCL7, CCL6, CXCL10, DOCK2, PLCB3, RAC2, PTK2B, CXCR4, PIK3R5, GNG5, LYN, NCF1, HCK, WAS, PRKCD, VAV1, CCL11, CCL12, GNGT2, CXCL16, CX3CR1	2.665
mmu05146:Amoebiasis	19	2.41E-04	IL1R1, GNA15, COL3A1, TLR2, ITGB2, COL5A3, COL5A2, ITGAM, TGFB1, PLCB3, LAMB2, COL1A2, IL1B, HSPB1, PIK3R5, COL1A1, COL11A2, CD14, FN1	2.650
mmu04650:Natural killer cell mediated cytotoxicity	17	5.88E-04	PTPN6, ICAM1, FCGR4, ITGB2, VAV1, CD48, RAC2, PTK2B, PLCG2, FCER1G, PIK3R5, FAS, IFNGR1, SYK, SH3BP2, TYROBP, LCP2	2.643
mmu05145:Toxoplasmosis	18	4.66E-04	GNAI2, TLR2, NFKBIA, H2-DMB1, H2-AB1, TGFB1, H2-DMB2, TNFRSF1A, IGTP, LAMB2, HSPA2, IL10RB, IL10RA, CASP8, H2-EB1, H2-AA, PIK3R5, IFNGR1	2.600
mmu05168:Herpes simplex infection	32	2.97E-06	TRAF1, CCL2, C3, TLR2, H2-D1, NFKBIA, CCL5, CD74, FOS, TNFRSF1A, TAP2, TAP1, CASP8, IL1B, FAS, IFNGR1, H2-K1, SP100, H2-M3, SOCS3, H2-Q1, H2-DMB1, H2-AB1, H2-Q8, H2-DMB2, IKBKE, CCL12, IRF7, JUN, H2-EB1, H2-AA, OAS1A	2.511

mmu04350:TGF-beta signaling pathway	13	0.005	BMP4, NBL1, CDKN2B, ID1, TGFBR1, TGFBR2, TGIF1, ID4, DCN, ID3, MYC, TGFB1, BMP6	2.496
mmu04974:Protein digestion and absorption	13	0.007	COL18A1, SLC1A5, COL9A3, COL3A1, COL1A2, COL6A2, COL6A1, COL1A1, COL11A2, COL5A3, COL5A2, KCNJ13, SLC7A7	2.411
mmu04664:Fc epsilon RI signaling pathway	10	0.022	LYN, RAC2, PLCG2, FCER1G, PIK3R5, INPP5D, VAV1, SYK, LCP2, BTK	2.400
mmu05164:Influenza A	25	1.05E-04	ICAM1, CCL2, SOCS3, NFKBIA, H2-DMB1, H2-AB1, CCL5, TLR7, H2-DMB2, CXCL10, IKBKE, CCL12, TNFRSF1A, HSPA2, JUN, IRF7, H2-EB1, PYCARD, IL1B, H2-AA, PIK3R5, OAS1A, FAS, MX2, IFNGR1	2.386
mmu00480:Glutathione metabolism	8	0.049	GPX1, GSTM2, GGT5, GPX3, ANPEP, GPX8, GPX7, MGST1	2.374
mmu04510:Focal adhesion	30	2.10E-05	TLN1, TNC, COL3A1, ITGB5, VTN, MYL9, LAMB2, RAC2, COL6A2, COL6A1, PIK3R5, COL11A2, THBS2, THBS3, SPP1, FN1, PARVG, TNXB, IGF1, MYL12A, FLNC, COL5A3, COL5A2, VAV1, FLNA, ITGA5, JUN, COL1A2, COL1A1, MYLK	2.365
mmu04630:Jak-STAT signaling pathway	21	4.91E-04	PTPN6, OSMR, CSF2RB2, SOCS3, IL6ST, IL21R, IL4RA, OSM, STAT6, CNTF, IL10RB, IL10RA, CSF2RB, CSF3R, PIK3R5, IL2RG, IL13RA1, MYC, CSF2RA, IFNGR1, IL3RA	2.364
mmu05322:Systemic lupus erythematosus	21	5.88E-04	HIST1H4N, HIST1H4M, HIST4H4, HIST1H2BC, C4B, C3, FCGR4, H2-DMB1,	2.332

mmu05166:HTLV-I infection	39	2.01E-06	H2-AB1, FCGR1, C1QC, H2-DMB2, HIST2H2AA1, C1QA, C1RA, C1QB, CD86, HIST1H2BN, H2-EB1, H2-AA, C2 IL1R1, TLN1, TSPO, SPI1, H2-D1, NFKBIA, ITGB2, NFKB2, TGFB1, TNFRSF1A, FOS, WNT4, CDKN2A, CDKN2B, CDKN2C, RRAS, IL2RG, PIK3R5, WNT6, MYC, H2-K1, EGR1, ZFP36, ICAM1, EGR2, LTBR, H2-M3, TGFBR1, TGFBR2, H2-Q1, H2-DMB1, H2-AB1, H2-Q8, H2-DMB2, FZD10, ATF3, JUN, H2-EB1, H2-AA	2.290
mmu05202:Transcriptional misregulation in cancer	23	4.61E-04	TRAF1, PLAT, CEBPA, CEBPB, TGFBR2, SPI1, IGF1, FCGR1, ITGAM, HHEX, CD86, BCL2A1D, NUPR1, BCL2A1B, CDKN2C, BCL2A1A, LYL1, IGFBP3, MYC, HPGD, CD14, PLAU, CSF1R	2.261
mmu04514:Cell adhesion molecules (CAMs)	22	8.27E-04	H2-K1, PTPRC, ICAM1, ICOSL, H2-M3, H2-Q1, H2-D1, H2-DMB1, ITGB2, H2-AB1, SDC4, ITGAM, PDCD1, H2-Q8, CLDN14, H2-DMB2, SIGLEC1, SDC1, CD86, H2-EB1, CD22, H2-AA	2.216
mmu00590:Arachidonic acid metabolism	12	0.019	GPX1, GGT5, CBR2, TBXAS1, PTGIS, PTGDS, GPX3, GPX8, LTC4S, GPX7, PLA2G2D, HPGDS	2.201
mmu05203:Viral carcinogenesis	28	8.31E-04	TRAF1, HIST1H4N, HIST1H4M, HIST4H4, IL6ST, C3, H2-D1, NFKBIA, NFKB2, CDKN2A, HIST1H2BN, CDKN2B, CASP8, CREB3L1, PIK3R5, ATP6V0D2, SYK, H2-K1,	1.978

			HIST1H2BC, LTBR, SP100, EGR2, H2-M3, LYN, H2-Q1, H2-Q8, IRF7, JUN	
mmu05162:Measles	16	0.019	TLR2, NFKBIA, TLR7, IKBKE, DOK1, HSPA2, FCGR2B, IRF7, IL1B, PIK3R5, IL2RG, MSN, FAS, OAS1A, MX2, IFNGR1	1.920
mmu05161:Hepatitis B	17	0.016	EGR2, TGFBR1, TLR2, NFKBIA, TGFB1, STAT6, FOS, IKBKE, PTK2B, JUN, IRF7, CASP12, CASP8, CREB3L1, PIK3R5, FAS, MYC	1.900
mmu05169:Epstein-Barr virus infection	24	0.006	TRAF1, H2-K1, ICAM1, LYN, H2-M3, FGR, H2-Q1, VIM, SPI1, H2-D1, NFKBIA, NFKB2, H2-Q8, CD44, HSPA2, IL10RB, JUN, RIPK1, IL10RA, PLCG2, HSPB1, PIK3R5, MYC, SYK	1.822
mmu04151:PI3K-Akt signaling pathway	38	7.47E-04	OSMR, CSF1, TNC, IL4RA, COL3A1, TLR2, ITGB5, VTN, EIF4EBP1, LAMB2, COL6A2, CSF3R, CREB3L1, COL6A1, IL2RG, PIK3R5, COL11A2, THBS2, GNG5, MYC, THBS3, CSF1R, SPP1, SYK, FN1, TNXB, NR4A1, IGF1, COL5A3, COL5A2, BCL2L11, OSM, GNGT2, ITGA5, LPAR6, COL1A2, COL1A1, IL3RA	1.767
mmu04810:Regulation of actin cytoskeleton	21	0.038	ITGB5, NCKAP1L, ITGB2, MYL12A, WAS, VAV1, ITGAM, IQGAP1, MYL9, ARPC1B, PFN1, EZR, ITGAX, RAC2, ITGA5, RRAS, PIK3R5, MSN, CD14, MYLK, FN1	1.602
mmu05200:Pathways in cancer	36	0.018	TRAF1, GNAI2, SPI1, NFKBIA, NFKB2, CXCL12, MMP2, TGFB1, FOS, PLCB3,	1.480

	WNT4, CDKN2A, LAMB2, RAC2, CDKN2B, CXCR4, CASP8, CSF3R, PIK3R5, FAS, WNT6, GNG5, MYC, CSF2RA, CSF1R, FN1, BMP4, CEBPA, TGFBR1, TGFBR2, IGF1, FZD10, GNGT2, LPAR6, JUN, PLCG2

These pathways are statistically significant (p <0.05).

Table 5. Enriched KEGG pathways identified to be significantly down-regulated in 8 weeks post-SCI.

Term	Count	*p* value	Genes	Fold Enrichment
mmu04721:Synaptic vesicle cycle	14	4.11E-09	DNM3, CPLX2, CPLX1, STXBP1, ATP6V1B2, STX1B, RIMS1, SLC32A1, SLC17A6, SLC18A3, UNC13C, SNAP25, NSF, DNM1	8.716
mmu04723:Retrograde endocannabinoid signaling	17	6.50E-09	ADCY3, GABRG2, ADCY1, GABRA1, GABRA3, MAPK10, KCNJ3, RIMS1, GRM1, SLC32A1, SLC17A6, PLCB4, KCNJ9, CNR1, MAPK9, MAPK8, GNG4	6.371
mmu00250:Alanine, aspartate and glutamate metabolism	6	0.002	GAD2, GOT1, ABAT, GAD1, RIMKLA, NAT8L	6.259
mmu05033:Nicotine addiction	6	0.003	SLC32A1, GABRG2, SLC17A6, GABRA1, GABRA3, CHRNA4	5.790

mmu04727:GABAergic synapse	12	1.28E-05	SLC32A1, ADCY3, GABRG2, GAD2, ADCY1, GABRA1, GABRA3, ABAT, GABBR2, GNG4, GAD1, NSF	5.324
mmu04728:Dopaminergic synapse	17	2.92E-07	SCN1A, DRD2, KIF5A, TH, KIF5C, MAPK10, KCNJ3, GNAL, PLCB4, KCNJ9, CALM3, MAPK9, MAPK8, GNG4, PPP2R2B, CALM2, AKT3	4.897
mmu04971:Gastric acid secretion	9	4.93E-04	ADCY3, ATP1B1, SSTR2, ADCY1, PLCB4, CCKBR, ATP1A3, CALM3, CALM2	4.825
mmu04930:Type II diabetes mellitus	6	0.009	MAPK9, MAPK8, MAPK10, MAFA, PRKCE, KCNJ11	4.632
mmu04970:Salivary secretion	9	7.76E-04	ADCY3, ATP2B2, ATP1B1, ATP2B3, ADCY1, PLCB4, ATP1A3, CALM3, CALM2	4.512
mmu04915:Estrogen signaling pathway	11	2.01E-04	ADCY3, ADCY1, PLCB4, KCNJ9, CALM3, GABBR2, SHC3, GRM1, KCNJ3, CALM2, AKT3	4.333

mmu05032:Morphine addiction	10	6.21E-04	SLC32A1, ADCY3, GABRG2, ADCY1, GABRA1, KCNJ9, GABRA3, GABBR2, GNG4, KCNJ3	4.151
mmu04261:Adrenergic signaling in cardiomyocytes	16	6.62E-06	ADCY3, ADCY1, ATP1B1, ATP1A3, CACNG2, CACNA2D3, TNNT2, ATP2B2, ATP2B3, PLCB4, CALM3, SCN4B, RAPGEF4, PPP2R2B, CALM2, AKT3	4.117
mmu04911:Insulin secretion	9	0.002	ADCY3, ATP1B1, ADCY1, PLCB4, ATP1A3, RAPGEF4, KCNJ11, SNAP25, KCNMB2	4.040
mmu04012:ErbB signaling pathway	9	0.002	NRG3, PAK3, MAP2K4, MAPK9, MAPK8, MAPK10, NRG1, SHC3, AKT3	3.993
mmu04912:GnRH signaling pathway	9	0.002	ADCY3, ADCY1, PLCB4, MAP2K4, MAPK9, CALM3, MAPK8, MAPK10, CALM2	3.948
mmu04713:Circadian entrainment	10	9.10E-04	ADCY3, ADCY1, PLCB4, NOS1AP, KCNJ9, CACNA1I, CALM3, GNG4, KCNJ3, CALM2	3.939
mmu05231:Choline metabolism in cancer	10	0.001	PDPK1, WASF3, DGKG, PIP5K1B, MAPK9, DGKK, MAPK8, SLC5A7, MAPK10, AKT3	3.822
mmu05014:Amyotrophic lateral	5	0.042	PRPH, SLC1A2, NEFH, NEFL, NEFM	3.784

sclerosis (ALS)				
mmu04940:Type I diabetes mellitus	6	0.021	GAD2, H2-T9, H2-BL, H2-T22, H2-Q6, GAD1	3.735
mmu04961:Endocrine and other factor-regulated calcium reabsorption	5	0.044	DNM3, ATP1B1, PLCB4, ATP1A3, DNM1	3.712
mmu04925:Aldosterone synthesis and secretion	8	0.007	ADCY3, ADCY1, PLCB4, CACNA1I, CALM3, PRKCE, CALM2, CAMK1D	3.591
mmu04725:Cholinergic synapse	10	0.002	ADCY3, ADCY1, PLCB4, CHRNA4, SLC18A3, SLC5A7, GNG4, KCNJ3, KCNJ14, AKT3	3.416
mmu04664:Fc epsilon RI signaling pathway	6	0.030	PDPK1, MAP2K4, MAPK9, MAPK8, MAPK10, AKT3	3.406
mmu05142:Chagas disease (American trypanosomiasis)	9	0.005	GNAL, ADCY1, PLCB4, MAP2K4, MAPK9, MAPK8, MAPK10, PPP2R2B, AKT3	3.373
mmu04750:Inflammatory mediator regulation of TRP channels	11	0.001	ADCY3, ADCY1, PLCB4, MAPK9, CALM3, MAPK8, ASIC1, MAPK10, PRKCE, HTR2C, CALM2	3.370

mmu04724:Glutamatergic synapse	10	0.003	ADCY3, SLC1A2, ADCY1, PLCB4, SLC17A6, GRM8, SHANK1, GNG4, GRM1, KCNJ3	3.357
mmu04024:cAMP signaling pathway	17	4.52E-05	ADCY3, ADCY1, ATP1B1, DRD2, ATP1A3, MAPK10, GABBR2, ATP2B2, SSTR2, ATP2B3, HTR1A, CALM3, MAPK9, RAPGEF4, MAPK8, CALM2, AKT3	3.331
mmu05218:Melanoma	6	0.036	E2F1, FGF18, FGF14, FGF13, FGF12, AKT3	3.262
mmu04020:Calcium signaling pathway	15	2.16E-04	ADCY3, ADCY1, CCKBR, TACR1, CACNA1I, TRHR, GRM1, GNAL, ATP2B2, ATP2B3, PLCB4, HTR7, CALM3, HTR2C, CALM2	3.217
mmu04917:Prolactin signaling pathway	6	0.040	TH, MAPK9, MAPK8, MAPK10, SHC3, AKT3	3.173
mmu04914:Progesterone-mediated oocyte maturation	7	0.024	PGR, ADCY3, ADCY1, MAPK9, MAPK8, MAPK10, AKT3	3.106
mmu04910:Insulin signaling pathway	11	0.003	PRKAR2B, PDPK1, PRKAR1B, MAPK9, CALM3, MAPK8, PRKAA2, MAPK10, SHC3, CALM2, AKT3	3.033

mmu04080:Neuroactive ligand-receptor interaction	22	1.28E-05	GABRG2, GLRB, GABRA1, CCKBR, DRD2, OPRL1, GABRA3, TACR1, TRHR, GLRA2, GABBR2, GRM1, NPY5R, SSTR2, HTR1A, GRM8, HTR7, CNR1, CHRNA4, ADRA2C, HTR2C, GRID1	2.980
mmu04022:cGMP-PKG signaling pathway	13	0.002	ADCY3, ATP2B2, ADCY1, ATP1B1, ATP2B3, PLCB4, ATP1A3, CALM3, ADRA2C, PRKCE, CALM2, AKT3, KCNMB2	2.935
mmu04921:Oxytocin signaling pathway	12	0.003	ADCY3, ADCY1, PLCB4, KCNJ9, CALM3, CACNG2, PRKAA2, CACNA2D3, KCNJ3, KCNJ14, CALM2, CAMK1D	2.932
mmu04015:Rap1 signaling pathway	16	4.00E-04	ADCY3, FGF18, ADCY1, MAGI3, FGF14, DRD2, EFNA3, FGF13, FGF12, PLCB4, CNR1, CALM3, RAPGEF4, EFNA5, CALM2, AKT3	2.886
mmu04014:Ras signaling pathway	17	2.65E-04	FGF18, FGF14, EFNA3, FGF13, FGF12, MAPK10, RASGRF2, PAK3, HTR7, CALM3, MAPK9, EFNA5, MAPK8, SHC3, GNG4,	2.866

			CALM2, AKT3	
mmu04071:Sphingolipid signaling pathway	9	0.015	PDPK1, PLCB4, SGPP2, MAPK9, MAPK8, MAPK10, PPP2R2B, PRKCE, AKT3	2.802
mmu04070:Phosphatidylinositol signaling system	7	0.039	IMPA2, PLCB4, DGKG, PIP5K1B, CALM3, DGKK, CALM2	2.786
mmu04972:Pancreatic secretion	7	0.044	ADCY3, ATP2B2, ATP1B1, ATP2B3, ADCY1, PLCB4, ATP1A3	2.702
mmu04726:Serotonergic synapse	9	0.021	HTR1A, KCND2, PLCB4, KCNJ9, HTR7, GNG4, HTR2C, KCNJ3, ALOX8	2.632
mmu04722:Neurotrophin signaling pathway	8	0.038	PDPK1, MAPK9, CALM3, MAPK8, MAPK10, SHC3, CALM2, AKT3	2.531
mmu05169:Epstein-Barr virus infection	12	0.023	POLR3G, YWHAG, YWHAH, H2-T9, H2-BL, MAP2K4, MAPK9, H2-T22, MAPK8, MAPK10, H2-Q6, AKT3	2.154
mmu04010:MAPK signaling pathway	14	0.014	FGF18, FGF14, MAP2K4, CACNA1I, FGF13, CACNG2, FGF12, MAPK10, CACNA2D3, RASGRF2, MAPK8IP2, MAPK9, MAPK8, AKT3	2.136

mmu04144:Endocytosis	14	0.027	DNM3, KIF5A, KIF5C, PIP5K1B, H2-Q6, TFRC, H2-T9, ZFYVE9, H2-BL, H2-T22, DNAJC6, IQSEC3, DNM1, SH3GL2	1.944

These pathways are statistically significant (p <0.05).

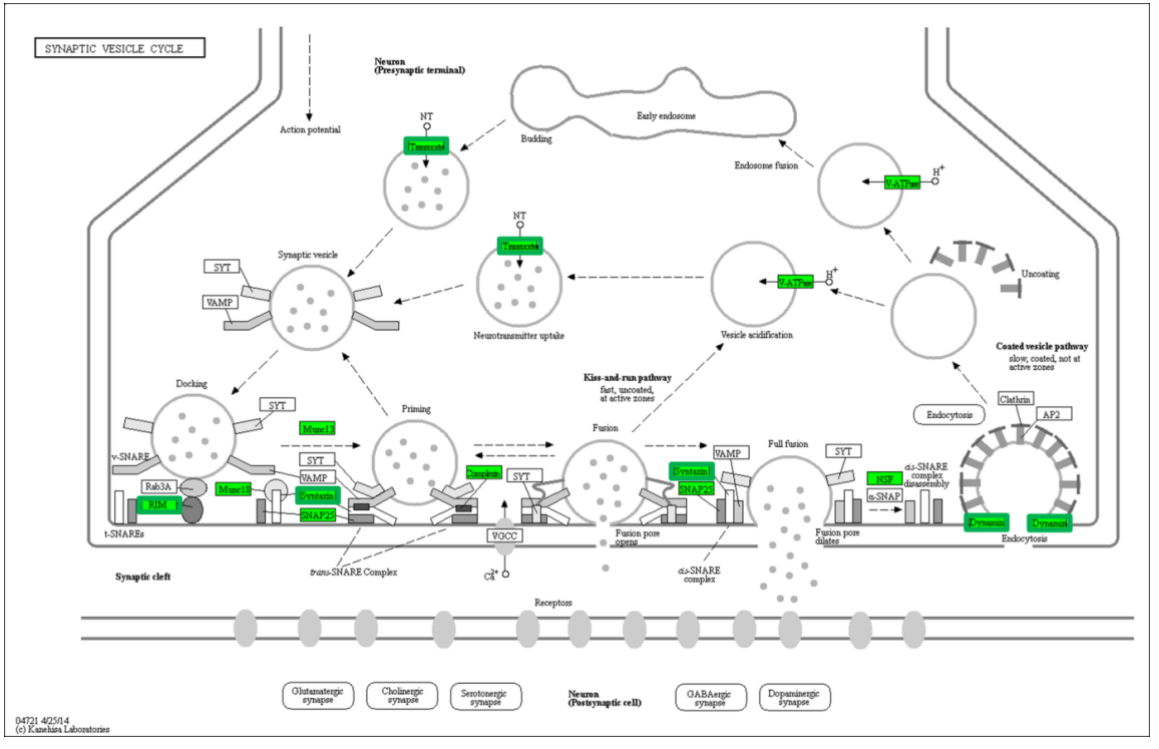

Figure 4. SVC pathway was identified as an enriched KEGG pathway in the SCI group. The genes were involved in the SCI group compared to the sham group at 2 weeks after injury represented as thick-green lines. The genes were involved in the SCI group compared to the sham group 8 weeks after injury as light-green covered boxes.

qRT-PCR validation with exposure to EE

The expression of target genes, such as *Slc17a6*, *Rims1*, *Stxbp1*, *Unc13c*, *Cplx1*, *Cplx2*, *Snap25*, *Stx1b*, and *Dnm1*, which are related in SVC, were validated by qRT-PCR with SCI-EE or SCI-Control for 2 and 8 weeks compared to sham (Figure 5). The expression of target genes was normalized to *GAPDH* expression and relative to the sham (indicated to dotted line and the expression value as 1.0 in the graph).

In the SCI-Control for 2 weeks, the expression of the target genes decreased compared to sham as follows: *Slc17a6* (0.736-fold), *Rims1* (0.917-fold), *Stxbp1* (0.584-fold), *Unc13c* (0.651-fold), *Cplx1* (0.843-fold), *Cplx2* (0.654-fold), *Snap25* (0.584-fold), *Stx1b* (0.688-fold), and *Dnm1* (0.602-fold). In the SCI-EE for 2 weeks, the expression of the target genes increased than SCI-Control for 2 weeks as follows: *Slc17a6* (0.821-fold), *Rims1* (0.954-fold), *Stxbp1* (0.938-fold), *Unc13c* (0.960-fold), *Cplx1* (0.908-fold), *Cplx2* (1.062-fold), *Snap25* (0.805-fold), *Stx1b* (0.855-fold), and *Dnm1* (0.788-fold). In particular, *Stxbp1*, *Unc13c*, *Cplx2*, and *Snap25* in SCI-EE showed statistically difference fold change with SCI-Control for 2 weeks as follows: *Unc13c* (p <0.001), *Cplx2* and *Snap25* (p < 0.01, respectively), and *Stxbp1* (p < 0.05).

As well as, in the SCI-Control for 8 weeks, the expression of the target genes decreased compared to sham as follows: *Slc17a6* (0.574-fold), *Rims1* (0.741-fold), *Stxbp1* (0.741-fold), *Unc13c* (0.522-fold), *Cplx1* (0.588-fold), *Cplx2* (0.216-fold), *Snap25* (0.839-fold), *Stx1b* (0.581-fold), and *Dnm1* (0.196-fold). In the SCI-EE for 8 weeks, the expression of the target genes increased than SCI-Control for 8 weeks as follows: *Slc17a6* (0.973-fold), *Rims1* (2.221-fold), *Stxbp1* (1.042-fold), *Unc13c* (0.757-fold), *Cplx1* (1.093-fold), *Cplx2* (0.786-fold), *Snap25* (1.037-fold), *Stx1b* (1.036-fold), and *Dnm1* (0.535-fold). In particular, all genes in SCI-EE showed statistically difference fold change with SCI-Control for 8 weeks as follows: *Slc17a6*, *Cplx1*, and *Stx1b* (p < 0.001, respectively), *Cplx2*

($p < 0.01$), and *Rims1*, *Stxbp1*, *Unc13c*, *Snap25*, and *Dnm1* ($p < 0.05$, respectively).

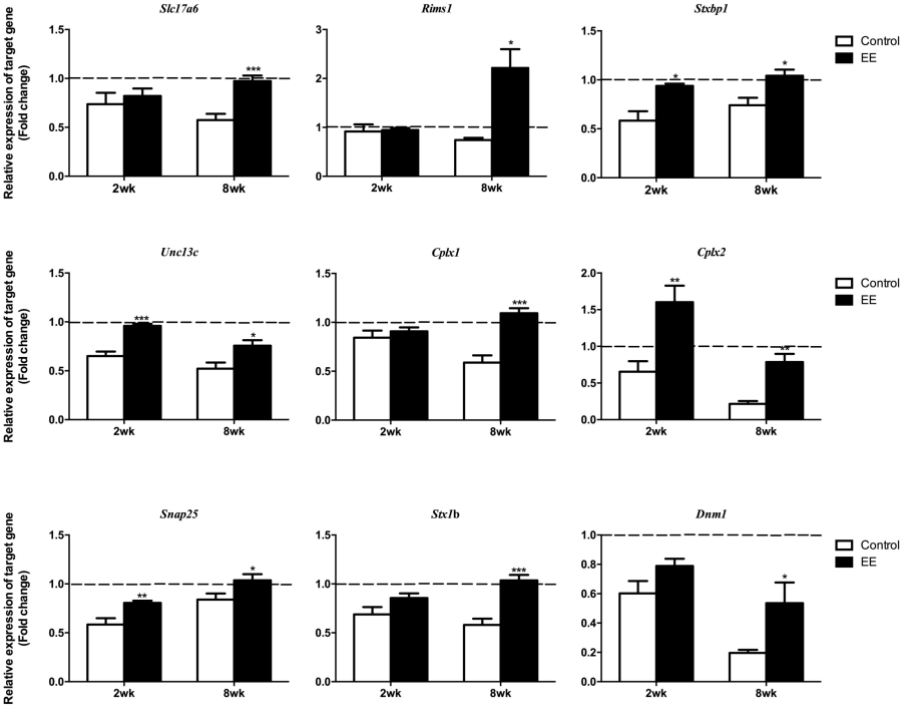

Figure 5. Validation of SVC-related genes after EE exposure by qRT-PCR. The relative expression of target genes for qRT-PCR was calculated using $2^{-\triangle\triangle Ct}$ method. All results were expressed as means ± SEM. The white box was indicated as SCI-Control, the black box was indicated as SCI-EE. The expression of target genes was relative to sham, and the expression values as 1 and represented in the graph as the dotted line.

Western blot and immunohistochemistry validation with exposure to EE

Slc17a6, Rims1/2, Stxbp1, Cplx1/2, Snap25, Stx1b, and Dnm1 were validated the protein level by Western blot with either SCI after exposure to EE or standard cages for 2 and 8 weeks compared to sham in Figure 6(A) and (B). It was

normalized to ACTIN expression and relative to sham (indicated to the dotted line and the protein value as 1.0 in the graph). In the SCI-Control for 2 weeks, the relative protein level was as follows: VGLUT2 (0.452-fold), RIM1/2 (0.571-fold), Munc18 (0.899-fold), Complexin-2 (1.226-fold), SNAP25 (1.163-fold), STX1B (0.864-fold) and DNM1 (1.075-fold). In the SCI-EE for 2 weeks, the relative protein level was as follows: VGLUT2 (1.025-fold), RIM1/2 (0.890-fold), Munc18 (0.964-fold), Complexin-2 (2.165-fold), SNAP25 (1.174-fold), STX1B (0.982-fold) and DNM1 (0.983-fold). In particular, the protein level of VGLUT2, RIM1/2, Complexin-2, and STX1B were statistically higher in SCI-EE than SCI-Control for 2 weeks as follows: VGLUT2, RIM1/2, and Complexin-2 ($p < 0.001$, respectively), and STX1B ($p < 0.05$).

As well as, in the SCI-Control for 8 weeks, the relative protein level was as follows: VGLUT2 (0.563-fold), RIM1/2 (1.873-fold), Munc18 (0.767-fold), Complexin-2 (1.707-fold), SNAP25 (0.715-fold), STX1B (0.938-fold) and DNM1 (1.023-fold). In the SCI-EE for 8 weeks, the relative protein level was as follows: VGLUT2 (0.883-fold), RIM1/2 (3.030-fold), Munc18 (0.953-fold), Complexin-2 (2.064-fold), SNAP25 (1.700-fold), STX1B (1.648-fold), and DNM1 (1.594-fold). All protein levels were statistically higher in SCI-EE than SCI-Control for 8 weeks ($p < 0.001$).

Immunohistochemistry of SNAP25 and syntaxin were conducted to investigate effects in SCI after exposure to EE for 8 weeks compared to standard cages for 8 weeks. The representative images of immunohistochemistry results (Figure 6 (C)) showed that the SNAP25+Syntaxin1+ cells count tended to increase in SCI after exposure to EE for 8 weeks compared to standard cages for 8 weeks (n=3). As well as, the percentage of SNAP25 and Syntaxin1-double positive cells was significantly increased in SCI after exposure to EE for 8 weeks compared to standard cages for 8 weeks (n=3) (Figure 6 (D)).

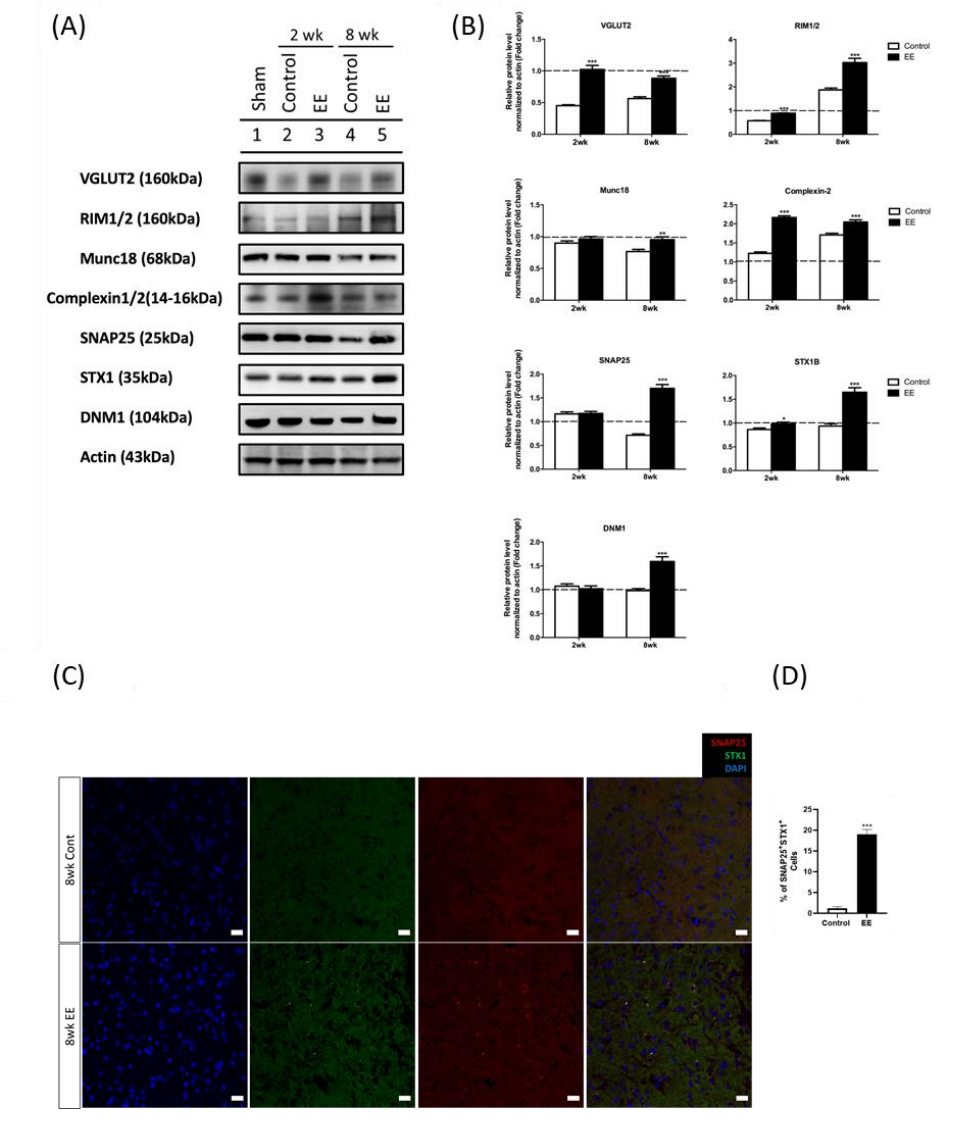

Figure 6. Validation of SVC-related genes after EE exposure by Western blot and immunohistochemistyr. (A) Western blot analysis was performed using antibodies against Slc17A6, Rims1/2, Munc18-1, Cplx1/2, SNAP25, Stx1B, DNM1 and Actin (a control). (B) Comparison of relative protein expression either SCI after exposure to EE (indicated as EE) or standard cages (indicated as control) for 2 and 8 weeks compared to sham. All results are expressed as means ± standard error of the mean (SEM) (* P <0.05, ** P <0.01 and *** P <0.001). (C)

Representative confocal microscopic images of SNAP25^{+}Syntaxin1^{+} cells in spinal cord. Scale bars 20 = μM. (D) The percentage of SNAP25 and Syntaxin1-double positive cells in spinal cord. All results are expressed as means ± standard error of the mean (SEM) (*** P <0.001).

Neurobehavior assessments with exposure to EE

In the BMS, the mean scores gradually increased after 3 days post-injury. After 14-, 42-, and 56-days post-injury, the BMS score was significantly greater in SCI-EE than SCI-Control (Figure 7 (A)). In the cylinder rearing test, the rearing count was significantly increased in SCI-EE at 8 weeks than SCI-Control (Figure 7 (B)). In the open field test, total zone and inner zone distances significantly increased in SCI-EE at 8 weeks than SCI-Control (Figure 7 (C) and (D)).

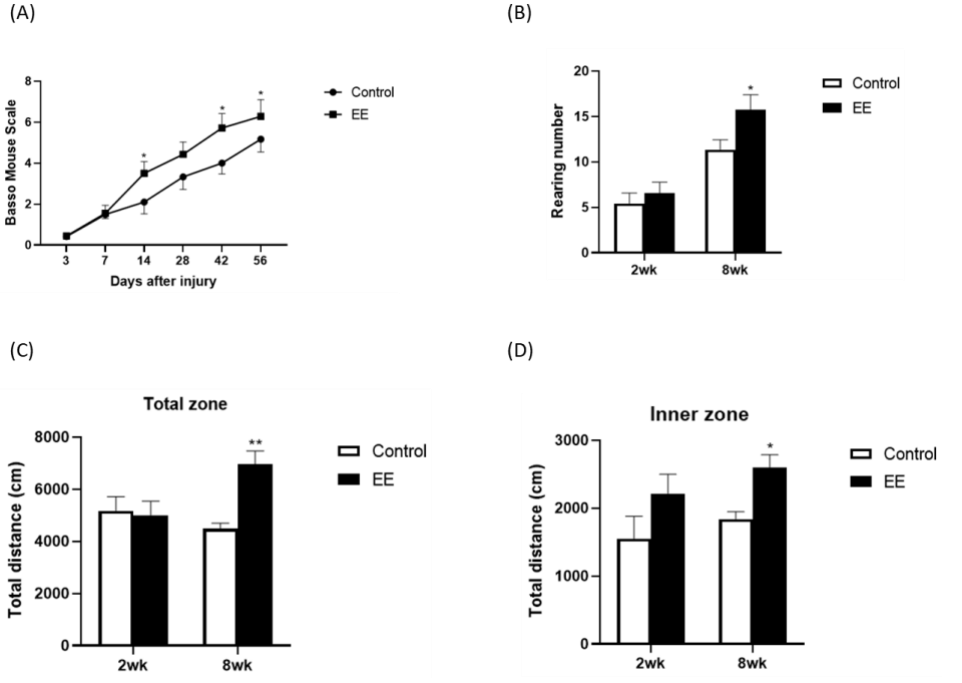

Figure 7. EE exposure improved neurobehavior function. (A) The BMS scores were obtained from day 3 to day 56 post-injury. (B) In the cylinder rearing test, the rearing count in SCI-EE compared to SCI-Control at 2 and 8 weeks. (C) Total

zone distance of the first interval in SCI-EE compared to SCI-Control at 2 and 8 weeks. (D) Inner zone distance of the first interval in SCI-EE compared to SCI-Control at 2 and 8 weeks. All results were expressed as mean standard error of the mean (SEM). n=4-5/group; *p<0.05, **p<0.01.

IV. DISCUSSION

To our knowledge, this is the first study to investigate the gene expression change after EE exposure in the SCI model. To explore the gene expression profile at the different time points after SCI and verify EE's therapeutic mechanism in the SCI mice model, we used RNA-sequencing, qRT-PCR validation, Western blot, and immunohistochemistry, and we performed neurobehavioral tests.

We found several enriched pathways in up-and-downregulated DEGs 2 weeks and 8 weeks after SCI. The SVC pathway, which we focused on identifying presynaptic plasticity after EE exposure, was down-regulated in the SCI group compared to the sham group at 2 weeks and 8 weeks after injury.

The synaptic vesicle cycle in the presynaptic terminal is divided into several sequential steps: (1) neurotransmitter are transported into synaptic vesicles (neurotransmitter uptake, *Slc17a6*), (2) synaptic vesicles moves to the active zone, (3) synaptic vesicles dock at the active zone (docking, *Rims1*, *Stxbp1*, *Unc13c*, *Snap25*, *Stx1b*), (4) docked vesicles are primed for fusion (priming, *Unc13c*, *Snap25*, *Stx1b*, *Cplx1*, *Cplx2*), (5) primed vesicles are fused with a synaptic membrane (fusion, *Snap25*, *Stx1b*), and (6) vesicles are endocytosed (endocytosis, *Dnm1*).[35] Among these down-regulated genes in our results, *Slc17a6*, *Rims1*, *Stx1b*, and *Dnm1* were down-regulated in 2 and 8 weeks after SCI. In SCI mice, down-regulation of SVC-related gene in RNA-sequencing reflects that synaptic function is decreased after SCI compared to sham.

In previous transcriptome studies in the SCI model, *Snap25* and *Stxbp1* are known as down-regulation during the acute phase of SCI.[20-24] On the other hand,

studies about presynaptic plasticity reported up-regulation of *Synapsin I, Synaptogyrin,* and *Synaptotagmin* during the acute phase and it was associated with spontaneous recovery.[18,19] However, in our transcriptome analysis, these genes were not found.

To identify whether EE could modulate SVC, we conducted qRT-PCR validation of down-regulated genes at 2 and/or 8 weeks after SCI, *Slc17a6*, *Rims1*, *Stxbp1*, *Unc13c*, *Cplx1*, *Cplx2*, *Snap25*, *Stx1b* and *Dnm1*. The expression results were compared SCI-EE with SCI-Control. In qRT-PCR validation, the same results as previous transcriptome study was seen. Genes are related to SVC were down-regulated in SCI compared with sham, but the expression pattern was different whether EE exposure or not.

Overall, every examined gene expression in SCI-EE was higher than SCI-Control at 2 and 8 weeks after SCI. Especially at 8 weeks after SCI, they showed significantly higher expression than SCI-Control. In addition, at 8 weeks after SCI, *Rims1*, *Stxbp1*, *Cplx1*, *Snap25*, and Stx1b showed higher gene expression than sham. It means that exposure to EE modulated the SVC in SCI mice, and changes caused by EE exposure were more prominent when prolonged exposure was provided.

Presynaptic plasticity is the modification of neurotransmitter release by synaptic vesicle fusion and priming, especially changes in the size of the pool of primed vesicle is thought as the critical mechanism.[10] So, in the SVC, steps before fusion are more important because of presynaptic plasticity. All examined genes, except *Dnm1*, which has the role in endocytosis, have the role in neurotransmitter uptake or docking and/or priming. Based on these results, we could assume that EE exposure leads to increased presynaptic activity (neurotransmitter uptake, docking, priming, fusion, and endocytosis) by modulating gene expression related to the SVC.

During priming and fusion, SNARE complex (SNAP25, syntaxin1 (STX1), and synaptobrevin) and complexin and Munc18, which bind to the SNARE complex,

have an essential role. *Snap25* and *Stx1b* encode SNAP25 and STX1, and *Stxbp1* (also known as *Munc18-1*) encode syntaxin-binding protein1 (SBP1, also known as Munc18).

Especially, complexin, which is encoded by *Cplx1* and *Cplx2*, is the only regulatory protein in synaptic vesicle cycle.[36] When complexin binds to SNARE complex, activation of prefusion SNARE complex is started. Complexin has a dual role in regulating synaptic vesicle exocytosis that it inhibits premature fusion of synaptic vesicle when endogenous neural activity is low, while promotes synaptic vesicle fusion by a depolarizing stimulus.[37,38] Synaptic strength is reduced in Cplx1 knock-out mice.[38] Increased expression of *Cplx1* and *Cplx2* compared to SCI-Control suggests regulating of synaptic vesicle exocytosis could be more effective in SCI-EE and also synaptic strength could be more favorable. *Snap25* encodes SNAP which is a t-SNARE protein, and it has the role in priming and fusion during synaptic vesicle cycle. Previous study found *Snap25* is down-regulated after SCI.[20-22,24] To up-regulate *Snap25* expression by overexpression recombinant vector enhance neurite outgrowth in spinal cord injured rats. And it is correlated with sensory functional improvement such as behavioral response to thermal and mechanical stimuli is improved.[39] In our study, expression of *Snap25* at 8 weeks after SCI increased in both SCI-EE and SCI-Control compared to 2 week after SCI. However, compared SCI-EE with SCI-Control at 8 weeks after SCI, *Snap25* was significantly increased in SCI-EE than SCI-Control. This statistical difference led to functional improvement in SCI-EE, and we could confirm in neurobehavioral assessment, BMS, cylinder rearing test, and open field test.

Glutamate, which is the major excitatory neurotransmitter, is transported into synaptic vesicles by vesicular glutamate transporters (VGLUTs), and VGLUT2 is encoded by *Slc17a6*. It shows pathway-specific expression in sensory processing, especially nociception.[40,41] Previous studies show heterozygous mice with VGLUT2 deficiency exhibit an absence or attenuated response of

mechanical and cold allodynia after spared nerve injury.[42,43] *Rims1* is encoded RIM1α and RIM1β which is a component of protein network in active zone. Active zone is the area were synaptic vesicles dock and fuse during release in presynaptic terminal. RIM1α and RIM1β are also essential for synaptic vesicle priming, and short- and long-term synaptic plasticity,[44-47] and especially RIM1α has the role in neuropathic pain after nerve injury.[48] In our study, *Slc17a6* and *Rims1* expression in SCI-EE at 8 weeks after SCI was significantly higher than SCI-Control while it was still decreased in SCI-Control. We could assume that allodynia could be increased in SCI-EE. However, we didn't check allodynia through this study, so we couldn't confirm this possibility.

Relative to the genes mentioned above, the study about synaptic plasticity of *Stx1b*, *Stxbp1*, and *Unc13c* is lacking. *Stx1b* encodes STX1B, and this protein binds with SNAP25, complexin, and syntaxin-binding protein1 (SBP1, which Stxbp1 encodes). Therefore, our study is meaningful in that it confirmed changes due to EE exposure of Stx1b, Stxbp1, and Unc13c, especially SNAP25 and Syntaxin, and proceeded to immunohistochemistry validation.

SBP1 is thought to have a role from initial docking to post-docking step.[49] *Unc13c* (also known as *Munc13-3*) encodes Munc13 proteins which regulates vesicle priming.[50] In previous study, *Unc13c* deficient mutant mice showed impaired ability to learn complex motor tasks.[51]

Dnm1 encodes dynamin1 which is involved endocytosis and implicated in synaptic vesicle recycling. So, role of this gens is somewhat differed to previous mentioned genes. But endocytosis is essential for starting of new synaptic vesicle cycle, we could assume that *Dnm1* is also contribute to synaptic plasticity.

V. CONCLUSION

In conclusion, our data provide evidence that exposure to enriched environments modulates synaptic vesicle cycle, neurotransmitter uptake, docking, priming, fusion, and endocytosis in mice with SCI. We also assume that presynaptic

plasticity might play a role in functional improvements in the EE group. And, if EE exposure is prolonged, a further synaptic plasticity process occurs.

REFERENCES

1. Lazarevic V, Pothula S, Andres-Alonso M, Fejtova A. Molecular mechanisms driving homeostatic plasticity of neurotransmitter release. Front Cell Neurosci 2013;7:244.
2. Fouad K, Tetzlaff W. Rehabilitative training and plasticity following spinal cord injury. Exp Neurol 2012;235:91-9.
3. Baldassarro VA, Sanna M, Bighinati A, Sannia M, Gusciglio M, Giardino L, et al. A Time-Course Study of the Expression Level of Synaptic Plasticity-Associated Genes in Un-Lesioned Spinal Cord and Brain Areas in a Rat Model of Spinal Cord Injury: A Bioinformatic Approach. Int J Mol Sci 2021;22.
4. Kazim SF, Bowers CA, Cole CD, Varela S, Karimov Z, Martinez E, et al. Corticospinal Motor Circuit Plasticity After Spinal Cord Injury: Harnessing Neuroplasticity to Improve Functional Outcomes. Mol Neurobiol 2021;58:5494-516.
5. Fischer F, Peduzzi J. Functional recovery in rats with chronic spinal cord injuries after exposure to an enriched environment. J Spinal Cord Med 2007;30:147-55.
6. Lankhorst A, ter Laak M, van Laar T, van Meeteren N, de Groot J, Schrama L, et al. Effects of enriched housing on functional recovery after spinal cord contusive injury in the adult rat. J Neurotrauma 2001;18:203-15.
7. Berrocal Y, Pearse DD, Singh A, Andrade CM, McBroom JS, Puentes R, et al. Social and environmental enrichment improves sensory and motor recovery after severe contusive spinal cord injury in the rat. J Neurotrauma 2007;24:1761-72.

8. Koopmans GC, Brans M, Gomez-Pinilla F, Duis S, Gispen WH, Torres-Aleman I, et al. Circulating insulin-like growth factor I and functional recovery from spinal cord injury under enriched housing conditions. Eur J Neurosci 2006;23:1035-46.
9. Starkey ML, Bleul C, Kasper H, Mosberger AC, Zorner B, Giger S, et al. High-Impact, Self-Motivated Training Within an Enriched Environment With Single Animal Tracking Dose-Dependently Promotes Motor Skill Acquisition and Functional Recovery. Neurorehabil Neural Repair 2014;28:594-605.
10. Rosenmund C, Rettig J, Brose N. Molecular mechanisms of active zone function. Curr Opin Neurobiol 2003;13:509-19.
11. Yang Y, Calakos N. Presynaptic long-term plasticity. Front Synaptic Neurosci 2013;5:8.
12. Regehr WG. Short-term presynaptic plasticity. Cold Spring Harb Perspect Biol 2012;4:a005702.
13. Pan L, Tan B, Tang W, Luo M, Liu Y, Yu L, et al. Combining task-based rehabilitative training with PTEN inhibition promotes axon regeneration and upper extremity skilled motor function recovery after cervical spinal cord injury in adult mice. Behav Brain Res 2021;405:113197.
14. Zhu H, Zhang J, Sun H, Zhang L, Liu H, Zeng X, et al. An enriched environment reverses the synaptic plasticity deficit induced by chronic cerebral hypoperfusion. Neurosci Lett 2011;502:71-5.
15. Lee M, Yu J, Kim J, Seo J, Park E, Kim C, et al. Alteration of synaptic activity-regulating genes underlying functional improvement by long-term exposure to an enriched environment in the adult brain. Neurorehabil Neural Repair 2013;27:561-74.
16. Bayat M, Sharifi MD, Haghani M, Shabani M. Enriched environment improves synaptic plasticity and cognitive deficiency in chronic cerebral hypoperfused rats. Brain Res Bull 2015;119:34-40.

17. Shin H, Kim H, Kwon M, Hwang D, Lee K, Kim B. Molecular and cellular changes in the lumbar spinal cord following thoracic injury: regulation by treadmill locomotor training. PLoS One 2014;9:e88215.
18. Gulino R, Dimartino M, Casabona A, Lombardo S, Perciavalle V. Synaptic plasticity modulates the spontaneous recovery of locomotion after spinal cord hemisection. Neurosci Res 2007;57:148-56.
19. Di Giovanni S, de Biase A, Yakovlev A, Finn T, Beers J, Hoffman E, et al. In vivon and in vitro characterization of novel neuronal plasticity factors identified following spinal cord injury. J Bio Chem 2004;280:2084-91.
20. Bareyre FM, Schwab ME. Inflammation, degeneration and regeneration in the injured spinal cord: insights from DNA microarrays. Trends Neurosci 2003;26:555-63.
21. Song G, Cechvala C, Resnick D, Dempsey R, Rao V. GeneChip analysis after acute spinal cord injury in rat. J Neurochem 2001;79:804-15.
22. Chen G, Fang X, Yu M. Regulation of gene expression in rats with spinal cord injury based on microarray data. Mol Med Rep 2015;12:2465-72.
23. Duan H, Ge W, Zhang A, Xi Y, Chen Z, Luo D, et al. Transcriptome analyses reveal molecular mechanisms underlying functional recovery after spinal cord injury. Proc Natl Acad Sci U S A 2015;112:13360-5.
24. Perkins JR, Antunes-Martins A, Calvo M, Grist J, Rust W, Schmid R, et al. A comparison of RNA-seq and exon arrays for whole genome transcription profiling of the L5 spinal nerve transection model of neuropathic pain in the rat. Mol Pain 2014;10:7.
25. Chomczynski P. A reagent for the single-step simultaneous isolation of RNA, DNA and proteins from cell and tissue samples. Biotechniques 1993;15:532-4, 6-7.
26. Kim M, Yu J, Lee M, Kim A, Jo M, Kim M, et al. Differential Expression of Extracellular Matrix and Adhesion Molecules in Fetal-Origin

Amniotic Epithelial Cells of Preeclamptic Pregnancy. PLoS One 2016;11:e0156038.

27. Won Y, Lee M, Choi Y, Ha Y, Kim H, Kim D, et al. Elucidation of Relevant Neuroinflammation Mechanisms Using Gene Expression Profiling in Patients with Amyotrophic Lateral Sclerosis. PLoS One 2016;11:e0165290.
28. Jiao X, Sherman B, Huang da W, Stephens R, Baseler M, Lane H, et al. DAVID-WS: a stateful web service to facilitate gene/protein list analysis. Bioinformatics 2012;28:1805-6.
29. Kanehisa M. Molecular network analysis of diseases and drugs in KEGG. Methods Mol Biol 2013;939:263-75.
30. Cho S, Suh H, Yu J, Kim H, Seo J, Seo C. Astroglial Activation by an Enriched Environment after Transplantation of Mesenchymal Stem Cells Enhances Angiogenesis after Hypoxic-Ischemic Brain Injury. Int J Mol Sci 2016;17.
31. Seo J, Yu J, Suh H, Kim M, Cho S. Fibroblast growth factor-2 induced by enriched environment enhances angiogenesis and motor function in chronic hypoxic-ischemic brain injury. PLoS One 2013;8:e74405.
32. Kim M, Yu J, Kim C, Choi J, Seo J, Lee M, et al. Environmental enrichment enhances synaptic plasticity by internalization of striatal dopamine transporters. J Cereb Blood Flow Metab 2016;36:2122-33.
33. Seo J, Kim H, Park E, Lee J, Kim D, Kim H, et al. Environmental enrichment synergistically improves functional recovery by transplanted adipose stem cells in chronic hypoxic-ischemic brain injury. Cell Transplant 2013;22:1553-68.
34. Livak K, Schmittgen T. Analysis of relative gene expression data using real-time quantitative PCR and the 2(T)(-Delta Delta C) method. Methods 2001;25:402-8.
35. Su¨dhof T. The synaptic vesicle cycle. Annu Rev Neurosci 2004;27:509-

47.

36. Trimbuch T, Rosenmund C. Should I stop or should I go? The role of complexin in neurotransmitter release. Nat Rev Neurosci 2016;17:118-25.

37. Martin JA, Hu Z, Fenz KM, Fernandez J, Dittman JS. Complexin has opposite effects on two modes of synaptic vesicle fusion. Curr Biol 2011;21:97-105.

38. Chang S, Reim K, Pedersen M, Neher E, Brose N, Taschenberger H. Complexin stabilizes newly primed synaptic vesicles and prevents their premature fusion at the mouse calyx of held synapse. J Neurosci 2015;35:8272-90.

39. Wang W, Wang F, Liu J, Zhao W, Zhao Q, He M, et al. SNAP25 ameliorates sensory deficit in rats with spinal cord transection. Mol Neurobiol 2014;50:290-304.

40. Schafer MK, Varoqui H, Defamie N, Weihe E, Erickson JD. Molecular Cloning and Functional Identification of Mouse Vesicular Glutamate Transporter 3 and Its Expression in Subsets of Novel Excitatory Neurons. J Bio Chem 2002;277:50734-48.

41. Wang ZT, Yu G, Wang HS, Yi SP, Su RB, Gong ZH. Changes in VGLUT2 expression and function in pain-related supraspinal regions correlate with the pathogenesis of neuropathic pain in a mouse spared nerve injury model. Brain Res 2015;1624:515-24.

42. Leo S, Moechars D, Callaerts-Vegh Z, D'Hooge R, Meert T. Impairment of VGLUT2 but not VGLUT1 signaling reduces neuropathy-induced hypersensitivity. Eur J Pain 2009;13:1008-17.

43. Moechars D, Weston MC, Leo S, Callaerts-Vegh Z, Goris I, Daneels G, et al. Vesicular glutamate transporter VGLUT2 expression levels control quantal size and neuropathic pain. J Neurosci 2006;26:12055-66.

44. Castillo PE, Schoch S, Schmitz F, Sudhof TC, Malenka RC. RIM1alpha

is required for presynaptic long-term potentiation. Nature 2002;415:327-30.

45. Calakos N, Schoch S, Sudhof TC, Malenka RC. Multiple roles for the active zone protein RIM1alpha in late stages of neurotransmitter release. Neuron 2004;42:889-96.

46. Kaeser PS, Kwon HB, Chiu CQ, Deng L, Castillo PE, Sudhof TC. RIM1alpha and RIM1beta are synthesized from distinct promoters of the RIM1 gene to mediate differential but overlapping synaptic functions. J Neurosci 2008;28:13435-47.

47. Schoch S, Castillo PE, Jo T, Mukherjee K, Geppert M, Wang Y, et al. RIM1alpha forms a protein scaffold for regulating neurotransmitter release at the active zone. Nature 2002;415:321-6.

48. Lai C, Ho Y, Hsieh M, Wang H, Cheng J, Chau Y. Spinal Fbxo3-Dependent Fbxl2 Ubiquitination of Active Zone Protein RIM1α Mediates Neuropathic Allodynia through CaV2.2 Activation. J Neurosci 2016;36:9722-38.

49. Meijer M, Burkhardt P, de Wit H, Toonen RF, Fasshauer D, Verhage M. Munc18-1 mutations that strongly impair SNARE-complex binding support normal synaptic transmission. Embo j 2012;31:2156-68.

50. Chen Z, Cooper B, Kalla S, Varoqueaux F, Young SM, Jr. The Munc13 proteins differentially regulate readily releasable pool dynamics and calcium-dependent recovery at a central synapse. J Neurosci 2013;33:8336-51.

51. Augustin I, Korte S, Rickmann M, Kretzschmar HA, Sudhof TC, Herms JW, et al. The cerebellum-specific Munc13 isoform Munc13-3 regulates cerebellar synaptic transmission and motor learning in mice. J Neurosci 2001;21:10-7.

ABSTRACT (IN KOREAN)

척수손상 쥐 모델에서 enriched environment 노출에 의한 시냅스 소포 사이클 조절

<지도교수 신지철>

연세대학교 대학원 의학과

유 지 현

enriched environment는 신체적, 인지적, 사회적 자극을 포함한 다양한 자극을 제공하여, 신경 회복 효과를 이끌어 내는 재활치료에 대한 동물 모델이다. enriched environment는 뇌척수 가소성을 촉진하여 동물 모델에서 운동 기능의 향상을 촉진 할 수 있다고 알려져 있으나, 척수손상모델에서 enriched environment에 의한 유전자 발현 차이이 및 전시냅스 가소성에 대한 효과는 아직 밝혀지지 않았다. 따라서, 본 연구에서는 척수손상 마우스 모델과 비손상 마우스 모델에서 유전자 발현의 차이를 확인한 후, enriched environment가 시냅스 소포 사이클 발현 및 전시냅스 가소성에 미치는 영향을 확인하고자 하였다.

이를 위해 생후 7주 된 마우스의 흉추 9번 부위의 척수를 압박 손상을 통해 척수손상을 유발하였으며, 비손상 마우스 모델은 같은 부위의 후궁절제술을 시행하였다. 이후 enriched environment

가 미치는 영향을 확인하기 위해, 척수손상 마우스를 enriched environment군과 대조군 (표준 사육환경경군)으로 나누어 총 8주간 사육하였다. 척수손상에 의한 유전자 발현의 차이를 확인하기 위해, 척수손상 2주 후와 8주 후에 유전자 발현 프로파일링 분석을 시행하였고, 1.5배 이상의 fold-change를 보이는 유전자를 분석하였다. 유전자 발현 프로파일링 분석 결과, 척수손상 2주 후에는 515개의 발현 증가된 유전자와 128개의 발현 감소된 유전자가 확인되었고, 8주 후에는 1,073개의 발현 증가된 유전자와 666개의 발현 감소된 유전자가 확인되었다. KEGG pathway 분석에서는 시냅스 소포 사이클이 척수손상 2주 및 8주에 모두 의미있게 감소되는 것을 확인하였다. 발현 감소가 확인된 시냅스 소포 사이클에 관계된 *Slc17a6, Rims1, Stxbp1, Unc13c, Cplx1, Cplx2, Snap25, Stx1b, Dnm1* 유전자들의 발현이 enriched environment 노출에 의해 어떤 차이를 보이는지 확인하고자 qRT-PCR과 Western blot 및 면역조직화학검사를 진행하였다. 또한, 쥐의 신경행동검사를 진행하여 enriched environment 노출에 따른 호전여부를 확인하였다. qRT-PCR 결과, 2주와 8주 모두 척수손상마우스 모델에서 대조군에 비해 높은 유전자 발현을 보였으며, 특히 8주에서는 통계학적으로 의미가 있는 높은 유전자 발현이 관찰되었다. 따라서, enriched environment 노출이 시냅스 소포 사이클 조절을 통해 전시냅스 가소성을 증가시킴을 확인하였다.

핵심되는 말 : enriched environment, 척수손상, 시냅스 소포, 신경가소성, 유전자 발현 프로파일링